Modeling Active Mechanosensing in Cell–Matrix Interactions

Bin Chen,[1] Baohua Ji,[2,*] and Huajian Gao[3,*]

[1]Department of Engineering Mechanics, Zhejiang University, Hangzhou 310027, China; email: chenb6@zju.edu.cn

[2]Biomechanics and Biomaterials Lab, Department of Applied Mechanics, Beijing Institute of Technology, Beijing 100081, China; email: bhji@bit.edu.cn

[3]School of Engineering, Brown University, Providence, Rhode Island 02912; email: huajian_gao@brown.edu

Annu. Rev. Biophys. 2015. 44:1–32

The *Annual Review of Biophysics* is online at biophys.annualreviews.org

This article's doi: 10.1146/annurev-biophys-051013-023102

*Corresponding authors

Keywords

receptor–ligand interaction, focal adhesion, stress fiber, cell traction, cell reorientation, multiscale modeling

Abstract

Cells actively sense the mechanical properties of the extracellular matrix, such as its rigidity, morphology, and deformation. The cell–matrix interaction influences a range of cellular processes, including cell adhesion, migration, and differentiation, among others. This article aims to review some of the recent progress that has been made in modeling mechanosensing in cell–matrix interactions at different length scales. The issues discussed include specific interactions between proteins, the structure and mechanosensitivity of focal adhesions, the cluster effects of the specific binding, the structure and behavior of stress fibers, cells' sensing of substrate stiffness, and cell reorientation on cyclically stretched substrates. The review concludes by looking toward future opportunities in the field and at the challenges to understanding active cell–matrix interactions.

Contents

INTRODUCTION

As the structural and functional unit of life, cells actively sense and respond to mechanical stimuli in their surroundings (140). The mechanical properties of the extracellular matrix (ECM), such as stiffness, surface topology, and deformation, are transduced into biochemical signals through interactions between the cell and the matrix; these interactions then regulate various cellular processes, including morphology, differentiation, motility, fate, and gene expression (19, 55, 65, 125). In general, cells adopt more rounded configurations on softer substrates, and spread into flatter, more pancake-like configurations on stiffer substrates (104). Matrix rigidity directs the differentiation of stem cells toward different lineage cell types (37), and neurons grow fastest on a matrix that has a stiffness similar to that of brain tissue (20). Cells migrate from softer to stiffer matrices, and their speed increases with the rigidity gradient (86, 155); they reorient themselves on cyclically stretched substrates in a direction nearly perpendicular to the direction of the stretch (73); and they distinguish between 2D and 3D environments in gene expression (124). The cell–matrix interaction also plays an essential part during development as cells evolve from a monolayer to a complex organism, with particular physical features associated with specific functions (83, 148).

Almost five decades ago interference reflection light microscopy was used to visualize cell–matrix adhesion in the form of discrete adhesion sites between fibroblasts and glass substrates (30). It was later recognized that these adhesion sites are located near the termini of contractile stress fibers (SFs), and physically couple the cytoskeleton to the ECM (67). At the molecular level, almost 200 different proteins, including integrin, vinculin, talin, paxillin, and tensin (17, 54), have been associated with cell–matrix adhesion (150). These proteins exist in multiple types and vary widely in structure and function (147). At the cellular level, cell–matrix interaction involves multiple subcellular structures, including focal adhesions (FAs), SFs, and microtubules, which collectively participate in cellular mechanotransduction (**Figure 1**) (127). Compared with adhesion problems in conventional engineering systems, a key feature of cell–matrix adhesion is that cells actively probe, pull, and push on the extracellular matrix.

In spite of recent developments in super-resolution fluorescence microscopy (70) and advanced bionanotechnology, understanding of the fundamental mechanisms of active mechanosensing in

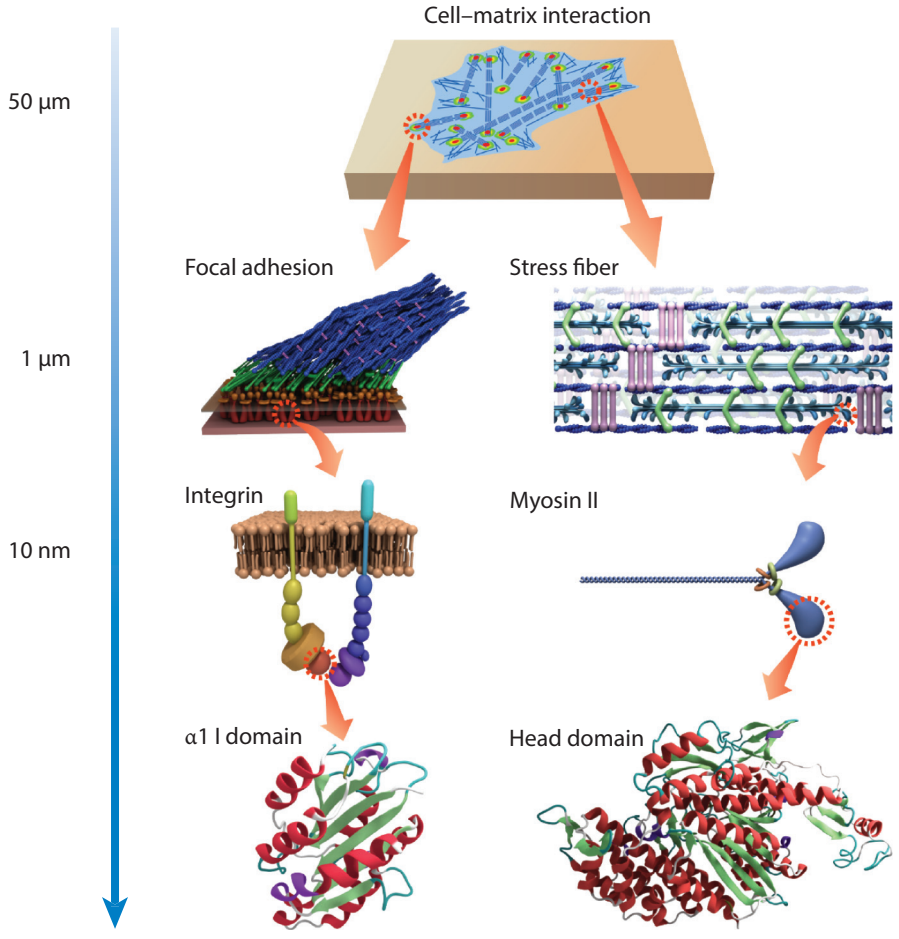

Figure 1

Schematics of stress fibers and focal adhesions—the main structures involved in cellular mechanosensing—and some critical components at multiple length scales.

cell–matrix interactions is still largely elusive. Although the total body of literature concerning cell–matrix interactions is rapidly growing, it is often focused on different scattered aspects or components of the problem, such as the structures and functions of individual proteins, FAs, and contractile SFs. The accumulative progress in the field calls for more efforts to be aimed at integrating different components of the problem into a more systematic and comprehensive understanding of active mechanosensing by cells.

The application of mechanics to the understanding of cellular phenomena is a burgeoning subject (14). This article aims to review, mainly from a mechanistic point of view, some of the recent progress made in modeling cell mechanosensing in cell–matrix interactions at multiple length scales. The issues to be discussed include specific interactions between adhesion proteins and mechanosensing at the molecular level, the structure and mechanosensitivity of FAs, the cluster effects of specific binding, the structure and behavior of SFs, cell sensing of substrate elasticity, the effect of cell shape on the distribution of traction force, the distance and depth that cells feel into a substrate, and cell reorientation on cyclically stretched substrates. The review

concludes with a look at future opportunities in the field, and the challenges to understanding active mechanosensing in cell–matrix interactions.

MECHANOSENSING AT THE MOLECULAR LEVEL

Mechanosensing in cells starts at the molecular level. In many cases, mechanical forces can induce conformational changes and expose the buried peptide sequences of a protein, open ion channels, and alter the dynamics of receptor–ligand binding (71). For example, integrins are adhesion molecules that mediate cell–cell and cell–matrix interactions (88, 156), as well as transmit signals bidirectionally across the plasma membrane (149) via receptor–ligand interactions, thereby playing a central role in mechanosensing during various cellular processes (**Figure 1**). Talin is a cytoskeletal molecule that directly connects integrin to cytoskeletal filaments (15, 72, 159) via multiple vinculin binding sites (60). The initially buried vinculin-binding sites within the talin rod can be exposed by mechanical forces for binding with vinculins; this activates a cascade of signals leading to the assembly and reorganization of the cytoskeleton (33). Mechanical forces can also unfold ligands, such as fibronectin, on the surface of the ECM (133). Such force-induced activation can be pervasive during signal transduction. For example, mechanical forces enable the phosphorylation of Cas in p130Cas, which then activates downstream signaling (123). Here we focus on the molecular interactions in FAs and SFs.

Molecular Components and Interactions Within Focal Adhesions

FAs are discrete regions of a cell that provide sites for mechanical attachment to the ECM (58). The attachment of FAs to the ECM is mediated by members of the integrin family of transmembrane proteins. Integrin-mediated adhesions are multiprotein complexes that link the extracellular matrix to the actin cytoskeleton (**Figure 1**). FA plaques at the cell–matrix interface connect SFs inside the cell to the ECM via a layer of transmembrane receptors that are primarily composed of integrins and probably also syndecans (98). Besides integrin, almost 200 different proteins are involved in FAs, including talin, tensin, α-actinin, paxillin, zyxin, vinculin, and a tyrosine kinase known as FAK (or focal adhesion kinase). It has been shown that the stretching of talin may have a major role in the integrin-mediated mechanosensing of focal adhesions (70a).

As a major force-bearing adhesion-receptor protein, integrin has a central role in adhesion-mediated cellular processes (109, 149a). During cell migration, integrins bind to the matrix at the leading cell edge, aggregate in the plasma membrane as part of increasingly strengthened adhesion complexes, then unbind, and are ultimately recycled (109). Within this bind–unbind mechanical cycle, integrins exhibit conformational changes that regulate their binding affinity, which depends on the mechanical force. Recent studies have shown that integrins have three conformational states: (*a*) a bent or low-affinity state, (*b*) a straight or intermediate-affinity state, and (*c*) a separating or high-affinity state featuring separation of their α and β subunit legs (109, 149). In the high-affinity state, integrins interact strongly with ligands on the ECM to form bonds, e.g., when they aggregate to promote the growth of FAs (26).

In their mechanical cycle, integrins are supposed to be first activated by the binding of talin with the intracellular tail of the β-subunit (109, 135). Once activated, they may form bonds with ligands on the matrix, and then the contractile force of the cytoskeleton may induce further conformational change of the integrins. The contractile force can alter the interdomain headpiece hinge via separation of the heterodimer legs as the β-subunit aligns along the force vector. In this scenario, a further increase in force will strengthen the FAs by accelerating the aggregation or clustering of integrins and associated adhesion proteins. Two generic molecular interactions that

depend on the applied force are critically important for the mechanosensing of FAs (79): One is the clustering of integrins and the associated adhesion proteins, and the other is the interaction between integrins and ligands on the ECM that forms the receptor–ligand bonds.

Molecular Components and Interactions Within Stress Fibers

Contractile SFs are collections of actin filaments formed by the contractile interaction of actin and myosin; they are bundled by cross-linking proteins, such as α-actinin (**Figure 1**). Large ventral SFs are anchored at both ends by FAs (69). This physical arrangement allows intracellular forces to be transmitted to the ECM, and extracellular forces to be transmitted to the cytoskeleton (87). Along the axis of SFs, regions containing the actin cross-linking protein α-actinin alternate with those containing myosin, and the polarity of the actin filaments is periodic. The nonmuscle form of the giant spring-like protein, titin or c-titin, also localizes to SFs in a periodic pattern. These observations are consistent with a sarcomeric structure similar to that of muscle fibrils, although SFs appear to be less ordered (134). A sarcomere is approximately cylindrical in shape, and an SF is built from many sarcomere units connected in series (134).

For SFs, a prominent example of mechanosensing at the molecular level is the force-controlled regulation of chemomechanical cycles of molecular motors, including nonmuscle myosin IIA, IIB, and IIC. Muscle myosin II undergoes an actin–myosin–ATP cycle, described by the Lymn–Taylor scheme, that comprises several stages (89). When myosins attach to the actin filament, molecular bonds are formed, similar to the receptor–ligand interaction. Within the power stroke of muscle myosin II, a light-chain binding region serves as a lever arm to amplify the movements of the converter domain (28). Without force constraint, the lever arm would swing all the way to complete the power stroke. However, if there is a force constraint, the swing can be arrested (52). For myosin II in skeletal muscle, it has been proposed that the swing of a lever arm is arrested at a transitional state when the motor force is approximately 6 pN (21), at which the reversible binding of P_i to the myosin head prevents ADP release (52). It has been argued that the swing being stuck at this translational state plays an important part in allowing the motor force to be self-regulated (21).

Modeling the Receptor–Ligand Interaction

The binding between a pair of receptor–ligand proteins is often mediated by weak but specific interaction via a lock-and-key mechanism. The dissociation of a specific bond is regulated by forces and often considered to be a thermally assisted escape over an energy barrier (42, 46). Because the dissociation rate of the bond depends on the applied force, there exist three categories of bond behaviors: (*a*) ideal bonds, with dissociation rates independent of the force; (*b*) slip bonds, with dissociation rates increasing as the force increases; and (*c*) catch bonds, with dissociation rates decreasing with increasing force.

For a slip bond, the dissociation rate, k_{off}, increases exponentially with the force according to Bell's law (8):

$$k_{off} = k_0 e^{f/f_0}, \qquad 1.$$

where f_0 is an intrinsic force scale and k_0 is the spontaneous dissociation rate in the absence of a force; $1/k_0$ typically ranges from a fraction of a second to around 100 s (46).

Under time-dependent forces, the stiffness of a molecular bond can strongly influence its lifetime. For example, for a bond being pulled at a constant velocity V, the force increases linearly with time as $f(t) = k_{LR}Vt$, where k_{LR} is the spring constant of the bond, and the mean lifetime of

the bond is (45):

$$T = \frac{1}{\mu k_0} e^{-1/\mu} E\left(\frac{1}{\mu}\right), \qquad 2.$$

where $\mu = k_{\mathrm{LR}} V / k_0 f_0$ and $E(x) = \int_x^\infty \frac{e^{-v}}{v} \mathrm{d}v$.

The strength of a bond is defined as the most frequently measured force at rupture, which, following Equation 1, is predicted to have a linear dependence on the logarithm of the loading rate (45):

$$f^* = f_0 \ln\left(\frac{KV}{k_0 f_0}\right). \qquad 3.$$

This prediction was verified by experimental measurements using a biomembrane force probe (44). The experiments showed a linear dependence of bond strength on the logarithm of the loading rate when extracting a test lipid molecule from a lipid bilayer. A similar trend was observed in the rupture of a biotin–streptavidin bond, albeit with a piecewise linear dependence due to the existence of multiple energy barriers (42) instead of a single energy barrier as assumed in Equation 1.

Equation 3 also predicts that the rupture force will diminish to zero or even negative value when the loading rate is vanishingly small. This is because Bell's model and similar models consider an irreversible rupture process and do not take into account bond rebinding (42). Therefore, such models may not be applicable at very low loading rates. To address this issue, Li & Ji (85) have recently reexamined the problem using Brownian dynamics simulations, and developed a new theoretical model by allowing bond rebinding. They treated bond rupture as the escape of a particle from a single energy well under external force (**Figure 2*a***), and showed that when the loading rate is lower than a critical value, bond rebinding dominates the rupture process, resulting in a rate-independent rupture force that corresponds to a nonzero bond strength at an ultralow loading rate (**Figure 2*b***). Notably, the rupture force increases with the loading stiffness, suggesting that the receptors and ligands would form stronger bonds on stiffer substrates leading to more

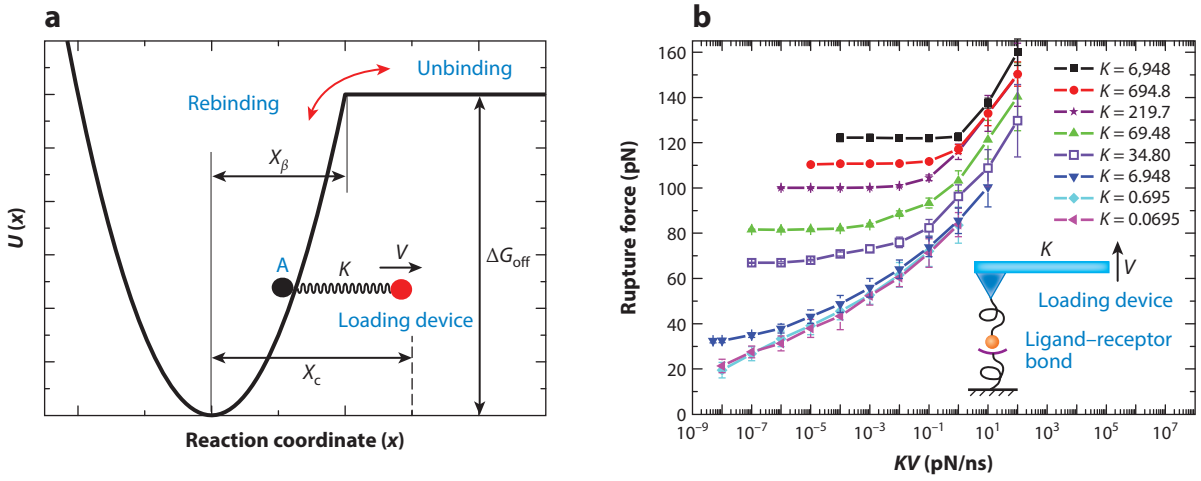

Figure 2

(*a*) Illustration of a particle, A, escaping from an energy well to mimic the rupture of the receptor–ligand bond under an external force. (*b*) Bond strength depends on the logarithm of the loading rate [obtained from Brownian dynamics simulations for different values of the spring constant *K* (pN/nm)]. Figure adapted from Reference 85 with permission.

stable cell adhesion when compared with softer substrates. This result provides further evidence for the mechanosensitivity of cell–matrix interactions at the molecular level.

In studying bond rebinding within a confined environment, Erdmann & Schwarz (40, 41) derived a relationship between the rebinding rate and the separation of a ligand–receptor pair as:

$$k_{on} = k_{on}^{0} \frac{l_{bind}}{Z} \exp\left(-\frac{k_{LR}\delta^2}{2k_B T}\right), \quad 4.$$

where k_B is Boltzmann's constant, T is the absolute temperature, k_{on}^{0} is a reference association rate when the receptor–ligand pair are within a binding radius l_{bind}, and Z is the partition function for a receptor confined in a harmonic potential between zero and δ. Qian et al. (112, 113) adopted this relationship to study the effect of substrate stiffness on the lifetime and strength of a cluster of receptor–ligand bonds between elastic media.

For catch bonds, the dissociation rate counterintuitively decreases with the applied force. These bonds, first proposed by Dembo et al. (34), have been reported in binding between FimH and mannose, L-selectin and endoglycan, P-selectin and P-selectin glycoprotein ligand-1, and myosin and actin (43, 62, 93, 122, 138), as well as between $\alpha_5\beta_1$ integrin and fibronectin (80). A number of theoretical models have been proposed for catch bonds, with dissociation following a single pathway, or two pathways, or even more complex modes (137a, 158). For example, assuming that a ligand escapes the receptor binding site via a catch pathway opposed by the force and a slip pathway promoted by the force, a formula for the dissociation rate of a catch–slip bond in a two-pathway model was derived as (106):

$$k_{off} = k_c e^{x_c f/k_B T} + k_s e^{x_s f/k_B T}, \quad 5.$$

where k_c and k_s are rate constants for unbinding through the catch and slip barriers with coordinates x_c and x_s, respectively, with x_c being negative.

MECHANOSENSING AT THE SUBCELLULAR LEVEL

Focal Adhesions

There are different forms of FAs. Nascent adhesions (focal complexes) appear as small dots 0.5–1 μm in size (10) within the lamellipodium; they have a lifetime on the order of seconds (147). They can either disassemble or mature into FAs depending on the mechanical forces (1, 25, 36, 69, 116). Mature FAs generally have an elongated shape 3–10 μm in length and several μm^2 in area (53, 67). The tension required to stabilize FAs is about a few nNs per μm^2 (6, 9). In some cases, FAs appear in the form of fibrillar adhesions (151, 152), as in fibronectin fibrillogenesis (91, 102). Other types of cell–matrix adhesion also exist, such as podosomes (118) or invadopodia (5, 59), which are mainly found in fast-moving cells, with invadopodia often existing in invading cells, such as tumor cells.

To understand the nucleation of FAs, Peng et al. (105) simulated the nucleation of integrin clusters using a kinetic Monte Carlo method, where integrin diffusion, activation, and the dynamics of receptor–ligand binding were considered. Their simulation indicated that high substrate stiffness would enhance the nucleation of FAs. Bihr et al. (13) studied the nucleation time and the critical number of receptor–ligand bonds needed for nucleation, accounting for the effect of membrane fluctuation. Shemesh et al. (131a) showed that the process of nucleation and growth of FAs is crucial to the formation of lamellipodium–lamellum interface in cell motility.

FAs can be induced to grow by mechanical force, such as by pulling the cell edge (116) or stretching the matrix adjoining the cell edge (76), and they undergo turnover when the force is relaxed. A model has been proposed to explain the mechanosensitivity of FAs (131) based on the hypothesis that stresses generated by pulling within a protein complex lower its chemical potential

(68). The model considered a 1D aggregate of identical molecules anchored on a substrate and subjected to pulling along the aggregation axis. The aggregate was assumed to exchange molecules with the surrounding medium at any point. Depending on the force level and distribution along the aggregate, a few modes of assembly were predicted, including disintegration, unlimited growth, unlimited growth after a critical length, and growth with a stable and finite steady-state length, in accordance with previous experimental observations (131). However, it was also found that when the SF assembly is selectively impaired while retaining a contractile lamella, the maturation of FAs as well as remodeling of fibronectin on the ECM is impeded, suggesting that tension is required but not sufficient for FA maturation without an SF template (101).

However, FAs can be disassembled when the force becomes too strong. To study the stability and disassembly of cell adhesion, a bond-cluster model is commonly adopted, in which the kinetics of bond breaking and reforming are considered using Bell's theory (8). Seifert (128) investigated the behaviors of a cluster of bonds subjected to linearly ramping forces. Erdmann & Schwarz (38, 39) adopted a one-step master equation approach to study the lifetime of a bond cluster. Their results suggest that an increase in the number of bonds enhances the stability of the cluster and many bonds together may have long-term and robust stability due to rebinding.

To investigate the effect of substrate stiffness on the lifetime and strength of FAs, Gao and coworkers (112, 113) developed a stochastic elasticity model of clusters of molecular bonds between two elastic media (**Figure 3**). A dimensionless parameter was identified as a controlling parameter to determine how the interfacial traction, $\sigma(x)$, is distributed within the adhesion domain between the cluster and substrate, which is written as follows:

$$\alpha = \frac{a\rho_{\mathrm{LR}}k_{\mathrm{LR}}}{E^*}, \qquad 6.$$

where a is the half-width of the adhesion cluster, and ρ_{LR} and k_{LR} are the bond density and stiffness, respectively; $E^* = 1/(\frac{1-v_c^2}{E_c} + \frac{1-v_s^2}{E_s})$ is the combined elastic modulus of cell and substrate, with v_c and v_s being the Poisson ratio and E_c and E_s the stiffness of cell and substrate, respectively. When $\alpha \to 0$, corresponding to a rigid substrate, the applied force is equally shared among all bonds within the cluster; in contrast, when $\alpha \to \infty$, corresponding to an extremely soft substrate, the distribution of bond force becomes highly nonuniform, with severe stress or force concentrated at the adhesion edges, suggesting that substrate rigidity has a strong effect on the strength and lifetime of the bond cluster.

Monte Carlo simulations have confirmed that the lifetime of a bond cluster can indeed be strongly affected by the rigidity of the substrate (**Figure 3*b***) (50, 113). The lifetime of a periodic array of clusters has been calculated as a function of cluster size for different values of substrate rigidity represented by E^*, with results indicating that there exists a size window for relatively stable adhesion. The simulations also showed that the lifetime of the cluster array can be regulated by the pulling angle. For a given magnitude of the applied loading, decreasing the pulling angle tends to stabilize the adhesion (**Figure 3*c***), suggesting there is a regulation mechanism that allows cells to switch between long- and short-lived adhesions by adjusting the pulling direction.

In addition to the stress-concentration effect, soft matrices also suppress rebinding in a bond cluster by increasing the local separation distance between open bonds (110). This has been demonstrated by showing that lifetime still varies with substrate rigidity when a uniform stress is directly applied to a bond cluster. It has been shown that the rebinding rate of an open bond anchored on two opposing elastic media is governed by the nondimensional parameter (50):

$$\chi = \sqrt{\frac{k_{\mathrm{LR}}}{2k_{\mathrm{B}}T}}\left(\frac{4}{E^*} + \frac{b}{k_{\mathrm{LR}}}\right)pb, \qquad 7.$$

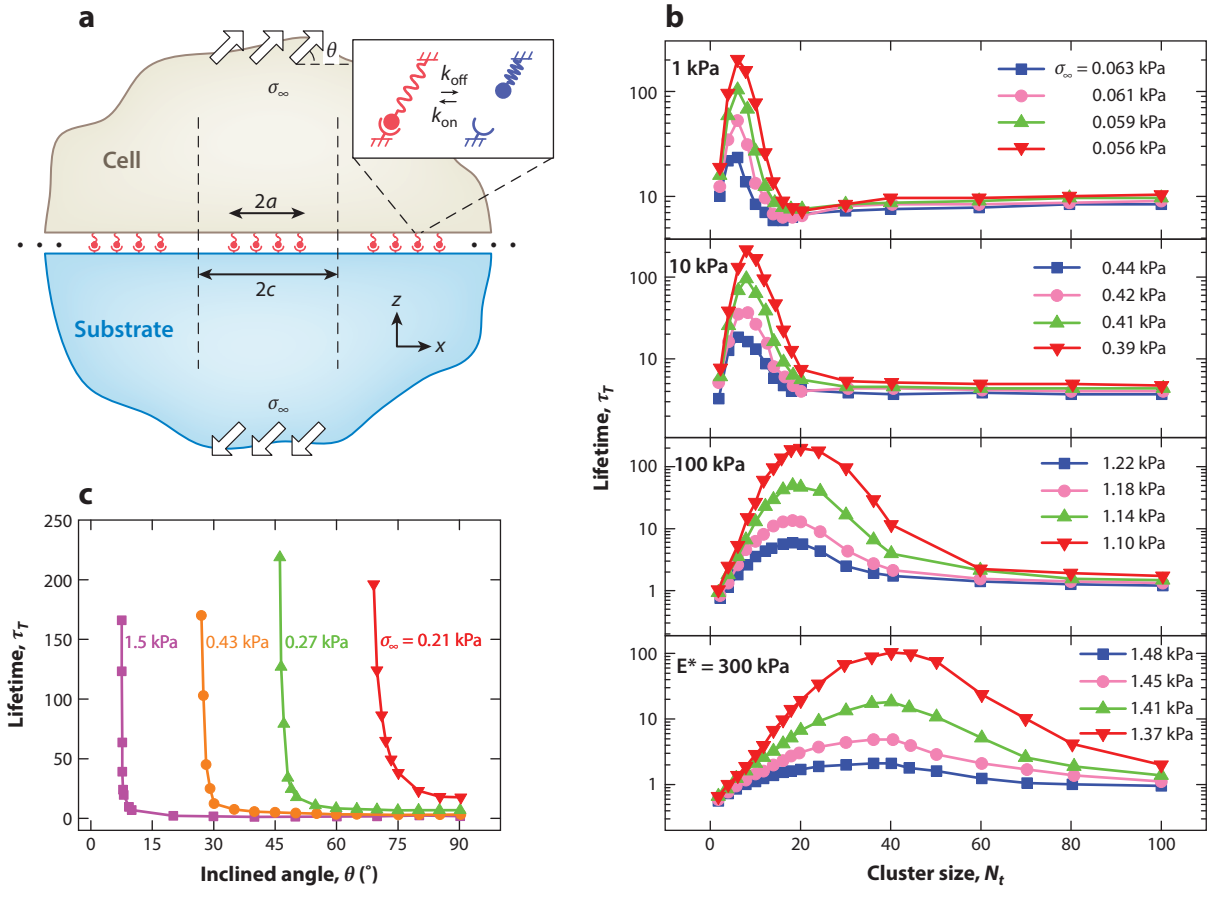

Figure 3

A mechanics model of cell adhesion illustrating the effect of adhesion size and cell–substrate elasticity on the adhesion lifetime: (*a*) schematic illustration of a periodic array of adhesion clusters between two dissimilar elastic media under an inclined tensile stress; (*b*) the lifetime of the periodic adhesion clusters as a function of the cluster size for different values of the reduced modulus E*; (*c*) the lifetime of the periodic adhesion clusters as a function of the pulling angle θ at various levels of applied stress. Adapted from Reference 113 with permission.

where p is the applied uniform stress on the cluster and b is the bond spacing, expressed in an exponential form as $\exp(-\chi^2)$. Therefore, the larger the χ, the smaller the rebinding rate. The mechanism by which an elastic modulus affects the rebinding rate is that on a soft substrate, the local surface separation due to the rupture of a pair of bonds is so large that rebinding becomes impossible, leading to a substantially shortened lifetime for the cluster. This result also suggests that the local stiff structure of an FA plaque (an assembly of nearly 200 different proteins) may have evolved from the necessity to maintain a stable adhesion cluster. However, the effect of substrate elasticity on adhesion lifetime could also be mitigated by pre-tension in the SFs. It has been demonstrated that pre-tension can shift the interfacial failure mode from crack-like failure towards uniform bond rupture and, thus, increase the lifetime of the cluster (23); this suggests that cell adhesion can be actively controlled by modulating the magnitude and pattern of myosin activities within the cytoskeleton.

According to Equation 7, the strength and lifetime of the molecular bonds in FAs can also be influenced by the spacing between neighboring bonds: the larger the spacing b, the larger the parameter χ, and the smaller the rebinding rate. This is qualitatively consistent with the experimental observations that FAs are inhibited and cells do not spread when ligand spacing is greater than 73 nm, but the formation of FAs and cells spreading to a pancake-like shape occur normally when ligand spacing is smaller than 58 nm (3, 4, 129). FAs are highly dynamic structures and their mechanical responses are biphasic with respect to the magnitude of applied forces: They grow under relatively small forces, but disassemble under relatively large ones. This biphasic behavior has been studied by Kong et al. (78, 79) using a microscopic model in which two generic molecular mechanisms were introduced, i.e., integrin clustering and integrin–ligand binding, both of which depend on mechanical force. Their results showed that there are two critical forces that determine the dynamics of FAs. The force-induced growth of FAs happens at a relatively small-scale force, which is dominated by the clustering of integrin and associated adhesion molecules. In contrast, the disassembly of FAs occurs at a relatively large-scale force, which is dominated by the binding dynamics of integrin–ligand bonds.

Stress Fibers

SFs are force-generating mechanotransducers in cells. There exist three types of SFs: ventral stress fibers, transverse arcs, and dorsal stress fibers within the cell (99) (**Figure 4*a***). Both ventral SFs and transverse arcs are composed of periodic distributions of myosin, α-actinin, and other cross-linking proteins on actin filaments, which make them contractile. In contrast, dorsal SFs are not contractile. SFs are also different in how they physically attach to FAs (99). Although ventral SFs are generally associated with FAs at both ends, transverse arcs are generally indirectly connected to the matrix via dorsal SFs, which attach to FAs at one end, with the other end rising toward the dorsal section of the cell (132). A ventral SF typically has a diameter of approximately 300 nm, a length of approximately 50 μm, a tension modulus of approximately 50 nN, and a pre-tensional load of a few nanoNewtons (32). An SF is built from many sarcomere units connected in series.

The intrinsic properties of SFs, such as pre-tension, viscoelastic relaxation, and motor-force homeostasis, are crucial to the mechanosensitive responses of cells to mechanical stimuli (23, 78, 114, 121, 157). It has been found that well-spread cells exert tension on their surroundings (35), which is caused mostly by the contractility of SFs. The existence of pre-tension has been demonstrated in isolated cells and their constituents, both directly (29, 82, 144) and indirectly (108, 145). For example, directly removing the tension in SFs by severing them with a laser caused the cut ends to retract (82, 87). When SFs were severed with femtosecond laser ablation, the length of the sarcomere decreased in an instantaneous elastic response, which was followed by a slower change in length due to myosin activity and viscoelasticity. Such retraction behaviors can be described by a viscoelastic cable model (82).

A mechanical model of sarcomere contraction that is consistent with experimental observation has been proposed, whereby an active element with tension generated by myosin is in series with a passive elastic element, and an impenetrable barrier prevents further sarcomere contraction (120). A model also has been developed to study the contractile behavior of SFs. The coupling between biochemistry and mechanics was taken into account with a system of reaction–diffusion equations in the model for inhomogeneous SF contraction occurring through the activation of myosin II motors along the Rho pathway. In this model, the sarcomere unit was simplified to a passive elastic spring, an active contractile module, and a viscous dashpot connected in parallel, and the whole SF was regarded as a string of such sarcomere units (11, 12), shown schematically in **Figure 4*b***. A quantitative analysis showed that protein localization and force were closely correlated in SFs and

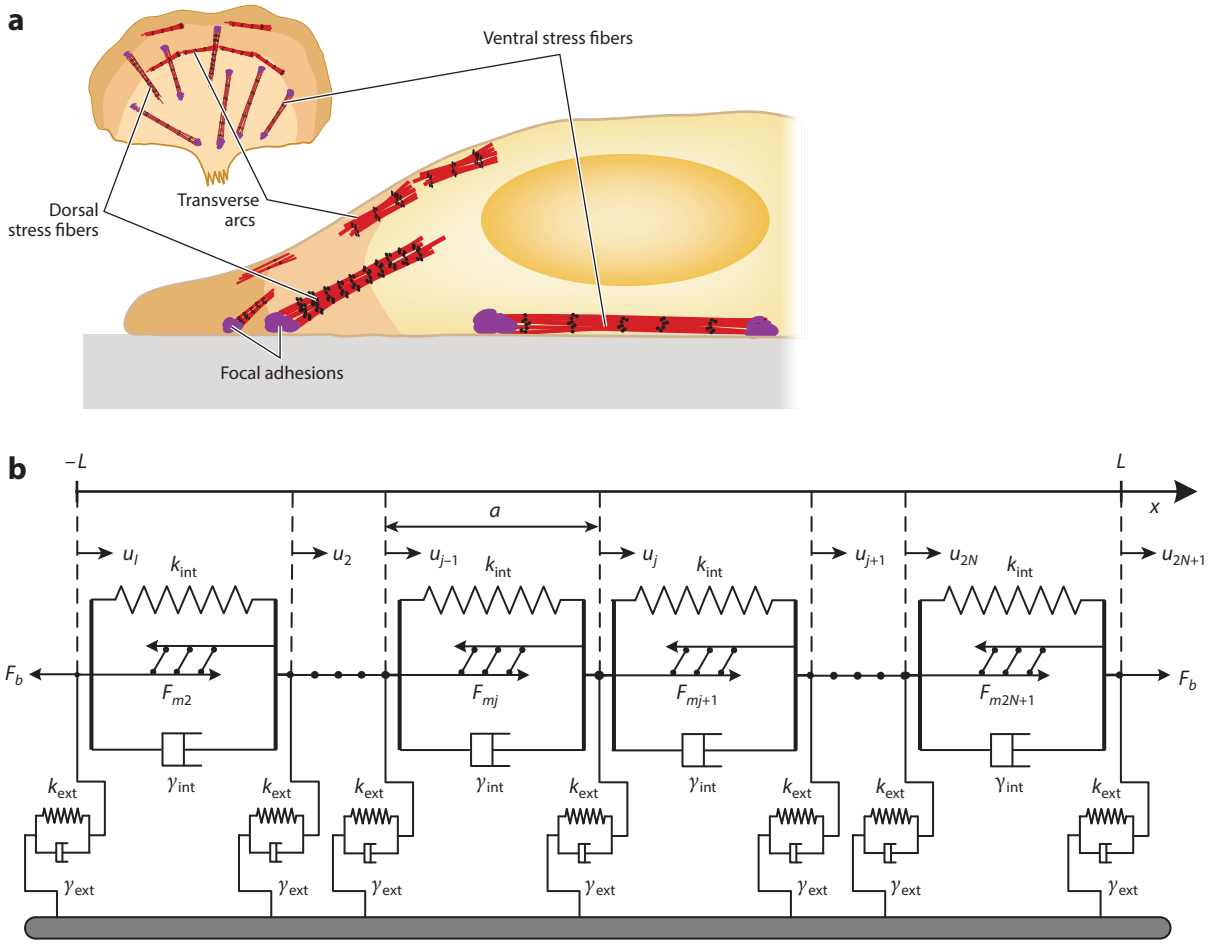

Figure 4

(*a*) Three types of stress fibers: dorsal stress fibers, transverse arcs, and ventral stress fibers. Panel adapted from MBInfo, National University of Singapore, available at **http://www.mechanobio.info**. (*b*) A viscoelastic mechanics model for stress fibers with inhomogeneous contraction. Panel adapted from Reference 11 with permission. Abbreviations: ext, exterior; int, interior.

suggested that a very direct force-sensing mechanism might exist along the length of an SF (27). For example, zyxin, a zinc-binding phosphoprotein that concentrates at FAs and along the actin cytoskeleton, was found to be recruited very quickly to substrate anchor points that were highly tensed upon SF release.

Owing to the structural similarity between an SF and a skeletal muscle fibril, a simple linear form of the empirical Hill's law, originally developed for muscle contraction, is often used to describe the relation between force F and contraction velocity V of an SF associated with myosin activity (12):

$$V = V_0\left(1 - \frac{F}{F_0}\right), \qquad 8.$$

where F_0 is the isometric force and V_0 a reference contraction velocity. A behavior of interest is motor-force homeostasis. Using the structural unit of a sarcomere, a molecular model for

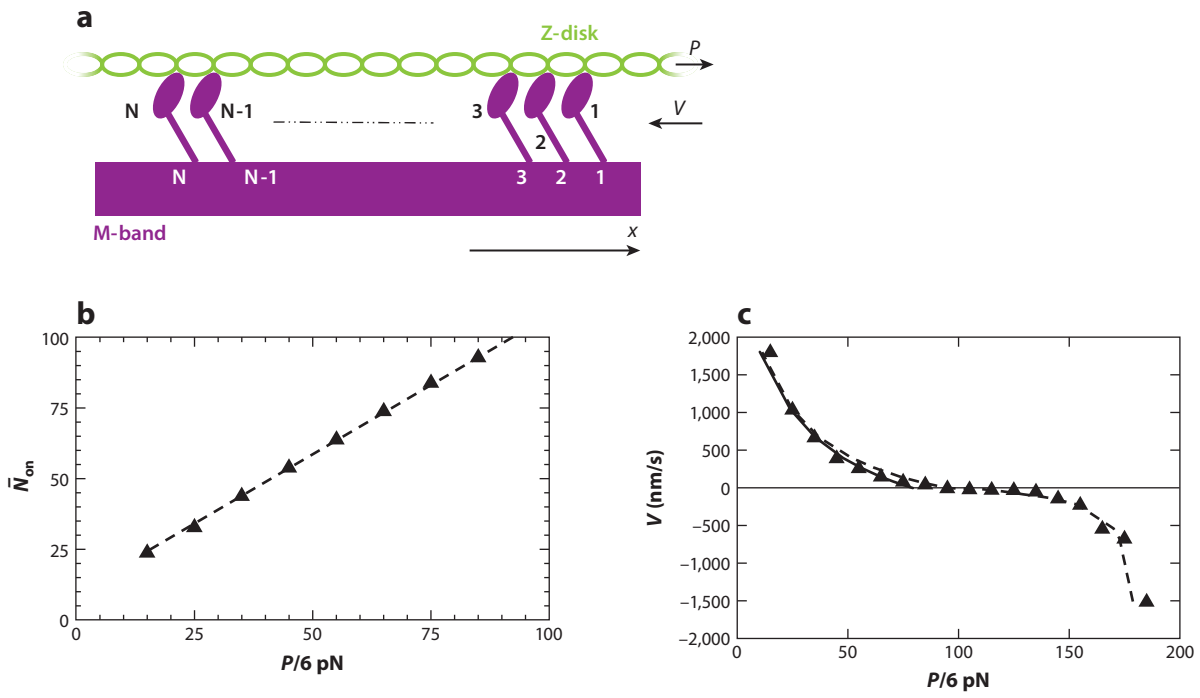

Figure 5

(*a*) Molecular model of a sarcomere during skeletal muscle contraction. The Z-disc is a structure existing between the dark lines (Z-lines) in electron micrographs of muscle fiber, and the M-band is a structure in the middle of a sarcomere. (*b*) The number of working motors increases linearly in proportion to the filament load, with force per motor at approximately 6 pN. (*c*) Simulated Hill's law for the contractile velocity of the actin thin filament versus the applied loads, with simulation results (*triangles*), fitted curve for the contractile part according to the equation $(P + 150)(V + 920) = \text{Constant}$ (*solid line*), and fitted curve with equation $P = 570[1-1.2V/(V + 650)]$ for the contractile part and $P = 630[1 + (15/\pi)\arctan(-12V/1800)]$ for the lengthening part (*dashed line*) (22). The units for P and V are pN and nm/s, respectively. Figure adapted from Reference 22 with permission.

SF contraction (**Figure 5*a***) was implemented within a coupled stochastic–elastic framework at two timescales (22). At the lower timescale, the system was considered elastic, and forces and displacements were solved using the finite element method; the results were then used to determine the reaction rates of motor binding and unbinding. The system's configuration was subsequently updated with a Monte Carlo method at the upper timescale. The simulation results indicated that the number of motors in the work state increases almost linearly with the filament load (**Figure 5*b***) and the motor force was regulated at approximately 6 pN, which is in agreement with other experimental data. The analysis indicated that the precise regulation of motor force in such an apparently chaotic system was due to both the stochastic feature and the force–stretch behavior of a single motor. The model has been further validated by recovering Hill's law between applied force and contractile velocity (**Figure 5*c***).

To investigate whether and how pre-tension in the cytoskeleton influences cell adhesion, Chen & Gao (23) developed a stochastic elasticity model of an SF attached to a rigid substrate via FAs. By comparing variations in adhesion lifetime and observing the sequences of bond breaking with and without pre-tension in the SF under the same applied force, they demonstrated that the effect of pre-tension is to shift the interfacial failure mode from crack-like propagation toward uniform bond failure within the contact region, thereby greatly increasing the lifetime of the adhesion.

This study suggests a feasible mechanism by which cell adhesion could be actively controlled via cytoskeletal contractility.

It has been postulated that the pre-strain in SFs is homeostatic and may be closely related to the overall pre-strain of the cell (66). It has been shown that SFs can shorten by approximately 15% within 1 s of being mechanically dislodged from a rigid substrate (82). Deguchi et al. (32) found pre-strain to be approximately 20%. Lu et al. (87) found that the pre-strain of SFs in endothelial cells increased from 10% to 26% when they were treated with 2 nM of calyculin A, a serine/threonine phosphatase inhibitor that elevates myosin light-chain phosphorylation; pre-strain decreased to 5% when they were treated with 10 μM blebbistatin, a selective inhibitor of actin–myosin interactions that has a high affinity for myosin II. These results indicate that SFs under isometric contraction exhibit a target tensional strain that is dependent on the degree of actin–myosin interaction.

MECHANOSENSING AT THE CELLULAR LEVEL

Experimental Observations

Cells actively probe their external environment and respond to various cues related to mechanical properties, such as stiffness, geometry, and dimensionality. In particular, substrate stiffness is recognized as playing a key part in the mechanosensing of cells. The stiffness of the human body varies from approximately 1 kPa in brain tissue to more than 1 MPa in bone. The stiffness of a particular tissue may also change with time, for example, due to aging or upon invasion by cancer cells (56, 103). There are many experimental reports concerning the effect of substrate stiffness on the behaviors of cells. Cells are more rounded on softer substrates, but spread out more like a pancake on stiffer substrates (57, 104, 137). Fibroblasts pull less on a softer matrix than on a stiffer matrix (86). In some studies, cells preferred to spread along the stiffest direction on a matrix patterned with anisotropic micropillars (57, 121). Most spectacularly, depending on the stiffness of the matrix, mesenchymal stem cells differentiate toward different cell types (37). Clearly, the stiffness of the ECM regulates many cellular behaviors, including morphology, adhesion, migration, and differentiation.

With newly developed experimental techniques, quantitative measurements of the mechanosensitivity of cells have been accumulating. For example, experiments have indicated that substrate stiffness has significant effects on both the traction forces at the cell–substrate interface and the area of a cell that is spread on the substrate surface. On a substrate patterned with arrays of microposts, Fu and coworkers (49, 146) observed that the cell-traction force, cell-spreading area, and total area of FAs all increased with the stiffness of the microposts, and the total traction force is linearly proportional to the cell-spreading area. Tan et al. (136) reported that the average force on the microposts increased as the cell-spreading area increased. Ladoux and coworkers (57, 121) found that the average force, as well as the strongest force, on a micropost both exhibit a biphasic dependence on the stiffness of the post; i.e., they increase linearly with the stiffness of the post when the post is relatively soft, but then level off to a plateau value on sufficiently stiff posts (**Figure 6*a***). On a continuous substrate, it has been reported that cell traction is proportional to the cell-spreading area (115); this area exhibits a similar biphasic dependence on the substrate stiffness (130). Such biphasic dependence of cell traction on substrate stiffness has not been satisfactorily explained. This lack of understanding has resulted in an ongoing debate about whether cells on an elastic substrate sense force or deformation (48, 121, 136).

In addition to its magnitude, the distribution of cell traction has also received considerable attention. Rape et al. (114) conducted a systematic study of the dependence of cell traction on

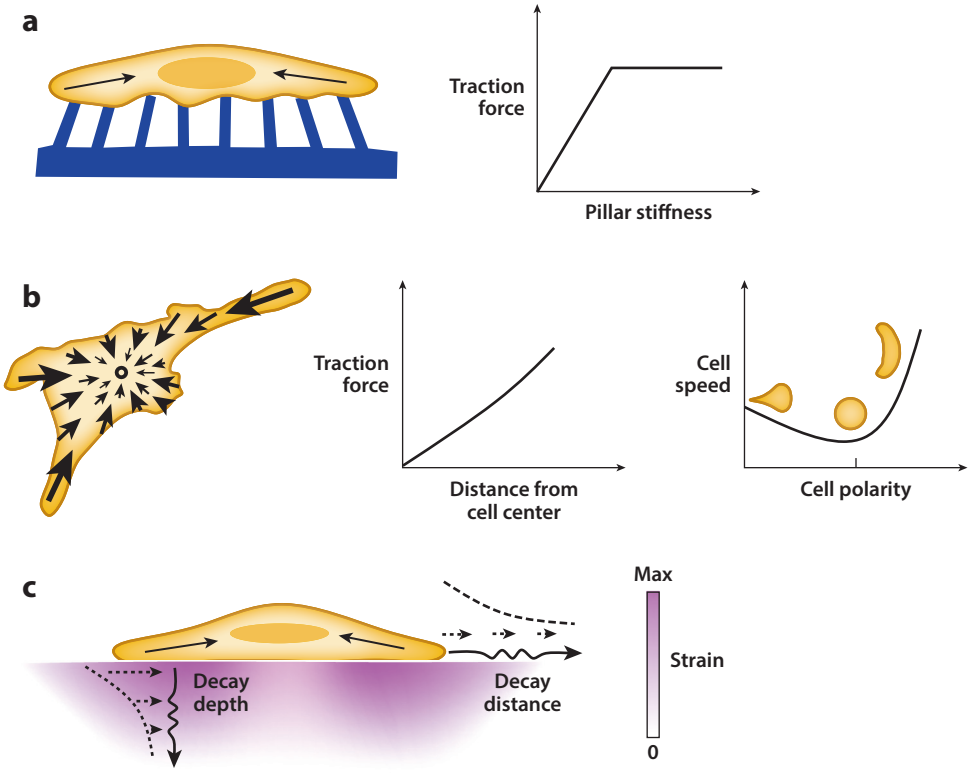

Figure 6

Representative mechanosensing events of cells on elastic substrates. (*a*) The cell exerts traction forces and deflects an array of elastomeric microposts on the substrate. Cell traction exhibits a biphasic dependence on the stiffness of the microposts. (*b*) The traction–distance law in cellular mechanosensing: the larger the distance from the cell center, the higher the cell traction. The commonly observed polarized cell shape is expected to play a crucial part in distributing the traction force and controlling cell-migration behaviors. (*c*) The cell-induced deformation field in the substrate decays with the depth or distance away from the cell. Figure adapted from Reference 66 with permission.

cell geometry and spreading area, and observed that cell traction and the size of FAs are both proportional to the distance from the cell center (**Figure 6*b***). Gardel et al. (51) and Dembo & Wang (35) showed that cell traction decreases in migrating keratocytes and fibroblasts as the distance from the cell edge increases. Similar relationships between traction and distance have been observed in cell colonies (96) and cells cultured in 3D matrices (84). A general observation is that the cell-traction force increases as distance from the cell center increases: the larger the distance, the higher the traction force. Surprisingly, until recently there has been relatively little discussion of the mechanisms underlying the observed relationship between force and distance (66), which may have important implications for the role of cell shape in regulating the distribution of traction and cell-migration behaviors (**Figure 6*b***).

In addition to the mechanical properties of the ECM, cells also actively respond to various external stimuli. For example, cells can sense deformation or force from the substrate (**Figure 6*c***). Some cells, such as vascular endothelial cells, are subject to cyclic loads under physiological conditions. It has been observed that upon cyclic stretch, initially randomly oriented cells on substrates rotate and reorient themselves almost perpendicularly to the loading direction (73, 100, 143).

The studies discussed above suggest that a few basic questions are critically important for understanding mechanosensitivity at the cellular scale.

- How does substrate stiffness influence the magnitude and distribution of cell traction?
- Why is cell traction distributed in a distance-dependent manner? What implications does this have for cell-migration behaviors? Can cell migration be controlled by regulating the distribution of cell traction?
- How far and how deeply can cells feel into a substrate?
- How do cells respond to the substrate's cyclic stretching?

Modeling the Cell–Matrix Interaction

Clarifying cell-traction force. He et al. (66) developed a contracting-disk model of cells interacting with an elastic substrate via adhesion molecules at the cell–substrate interface (**Figure 7**). To enable the model to be as simple as possible without losing the essential physics of the problem, they treated an adherent cell as a pre-strained elastic disk with the following constitutive equation:

$$\sigma_{ij} = \frac{E_c}{1+\nu_c}\left(\varepsilon_{ij} + \frac{\nu_c}{1-\nu_c}\varepsilon_{kk}\delta_{ij}\right) + \frac{E_c}{1-\nu_c}\varepsilon_0\delta_{ij}, \qquad 9.$$

where E_c is Young's modulus; ν_c is Poisson's ratio of the cell; and $i, j = 1, 2$ are coordinates in the plane of the disk. The second term on the right-hand side of the above equation accounts for cytoskeletal contractility.

The cell traction $\tau_c(r)$ at the interface is related to the elongation $\Delta_r(r)$ of molecular bonds as:

$$\tau_c(r) = \rho k_b \Delta_r(r), \qquad 10.$$

where ρk_b is the areal stiffness of the interfacial bonds, and ρ and k_b denote bond density and bond stiffness, respectively; $\Delta_r(r) = u_s(r) - u_c(r)$; and $u_c(r)$ and $u_s(r)$ are the displacements of the cell and substrate at the interface, respectively (**Figure 7**).

For a semi-infinite substrate, He et al. (66) derived a perturbation solution for the traction force between cell and substrate, as well as deformation in the cell and substrate. It was shown that the solution is governed by two dimensionless parameters: $a = \frac{2\rho k_b R}{\pi E_s^*}$ and $b = \frac{\rho k_b R^2}{E_c^* h_c}$, where R is the cell size, h_c is the cell thickness, E_c^* and E_s^* represent $\frac{E_c}{1-\nu_c^2}$ and $\frac{E_s}{1-\nu_s^2}$, respectively, where E_s and ν_s denote Young's modulus and Poisson's ratio of the substrate, respectively. Here the mechanical properties of the substrate should be interpreted as the effective properties of the substrate coupled with an adhesive protein layer to which the cell is attached (139a).

The zeroth-order solution of the traction, corresponding to cells adhering to a rigid substrate, is:

$$\bar{\tau}_{c(0)}(\bar{r}) = -\frac{h_c b}{R} C_{1(0)} \mathrm{BesselI}(1, \sqrt{b}\bar{r}). \qquad 11.$$

For a substrate of finite thickness, an approximate solution of cell traction was derived as:

$$\bar{\tau}_c = -\frac{h_c}{R}[C_1 A^2 C \mathrm{BesselI}(1, A\bar{r}) + C_2 B^2 D \mathrm{BesselI}(1, B\bar{r})], \qquad 12.$$

where A, B, C, C_1 and C_2 are constants whose detailed expressions can be found in (66). Note that in He et al.'s study (66) the traction is assumed to be along the horizontal direction, and the vertical force between the cell and the substrate is neglected. This assumption is reasonable for a relatively stiff substrate. For a very soft substrate (much softer than a cell), the measurements from Legant et al. (83a) have shown that the vertical component of cell traction can be as large as 30–50% of the horizontal component. Nevertheless, the theory of He et al. captured the essence

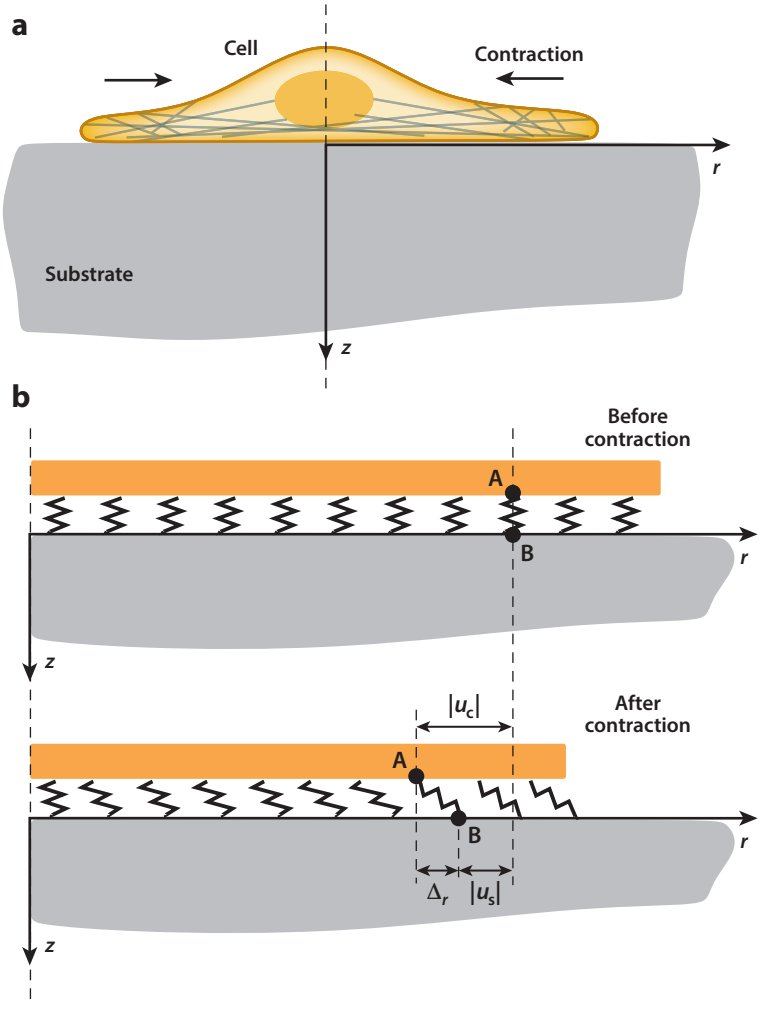

Figure 7

The contracting-disk model of cell–matrix interaction. (*a*) Schematic of a cell adhering to and pulling on an elastic substrate, owing to the intrinsic contractility of the cell. (*b*) The cell is modeled as an elastic contracting disk that is anchored to the substrate via molecular bonds (treated as elastic springs) at the cell–substrate interface. r and z are radial and vertical coordinates, respectively, u_c and u_s are displacements of the cell and substrate, respectively, and $\Delta_r = u_s - u_c$. A and B are the points on the surface of the cell and substrate, respectively, connected by a molecular bond. Figure adapted from Reference 66 with permission.

of the mechanics of cell–matrix interactions, and their predictions show broad agreement with experiments (66). For instance, it was predicted that horizontal traction alone could induce vertical displacement on the substrate, which is consistent with experimental measurements (83a, 94a).

Effect of substrate stiffness: Do cells sense force or deformation of their substrates? Substrate stiffness has a significant effect on cell displacement and traction. For example, cell displacement varies linearly with distance on a soft substrate, but it varies exponentially on a stiff substrate. Cell traction also varies linearly with distance near the center on a soft substrate,

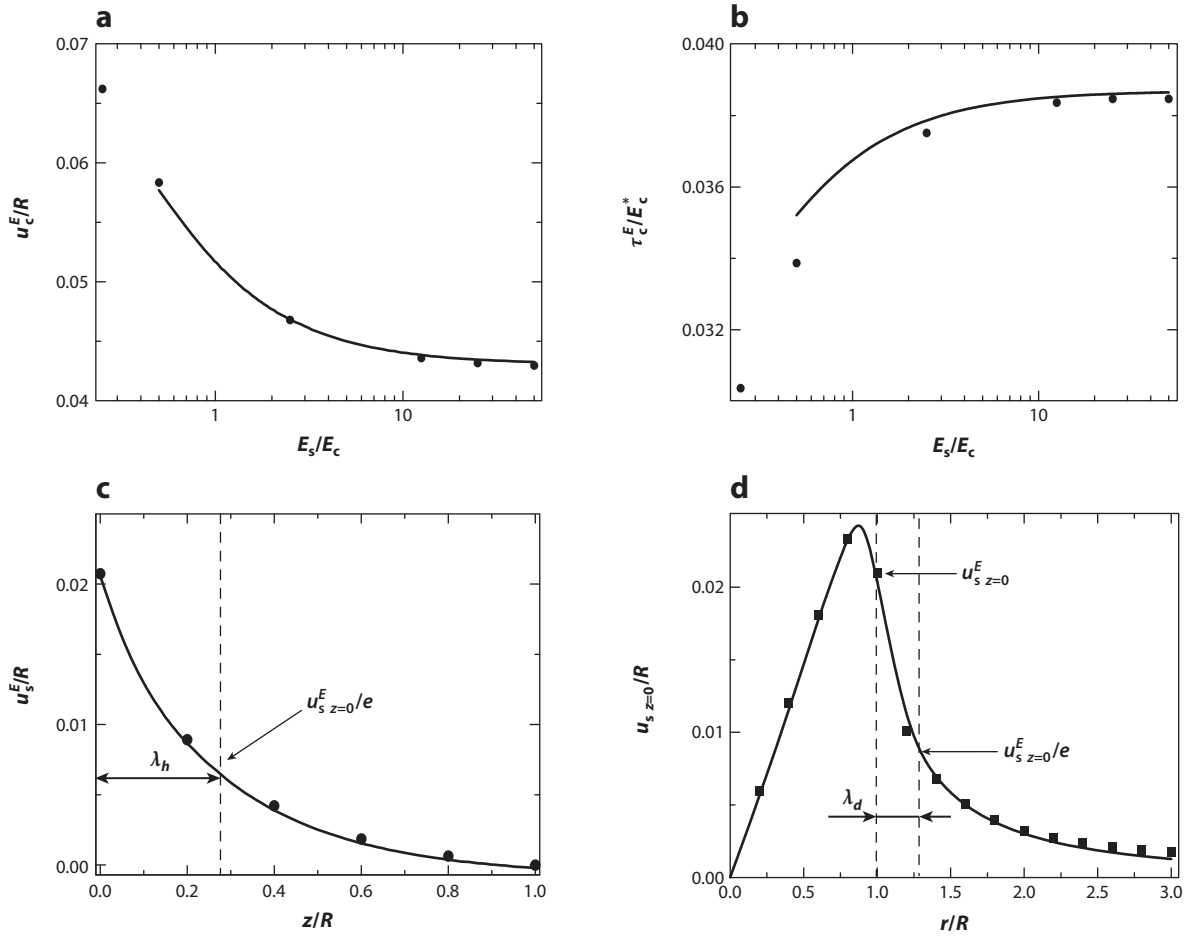

Figure 8

Cell-induced elasticity and deformation occurring during interaction with a substrate. (*a*) Cell displacement is inversely proportional to substrate stiffness when the stiffness is low, but it decreases to a plateau value when the stiffness is high. (*b*) Cell traction also exhibits a biphasic dependence on substrate stiffness. (*c*) Variations of radial displacement at the cell edge, with depth z into the substrate, λ_h being the characteristic depth of decay. (*d*) Variation in radial displacement on the substrate surface with distance from the cell center, λ_d being the characteristic lateral distance of decay from the cell edge. Figure adapted from Reference 66 with permission.

but it rises dramatically at the cell's periphery. Particularly, the results from the contracting-disk model indicate that peripheral cell displacement is inversely proportional to substrate stiffness for $E_s/E_c < 5$, and that it asymptotically settles to a plateau for $E_s/E_c > 5$ (**Figure 8*a***). In comparison, cell traction first increases and then levels off to a constant value with increasing substrate stiffness (**Figure 8*b***). These results suggest that cells cannot sense changes in substrate stiffness once it rises above a critical value (66). Similar conclusions had been reached earlier based on a simple two-spring model (126). In that model, the interfacial bonds and substrate are modeled as two elastic springs connected in series, with an overall effective stiffness of $k_{eff} = k_b k_s/(k_b + k_s)$, k_s being the effective spring constant of the substrate, and k_b the effective spring constant of the interfacial bonds. If $k_s \gg k_b$, then $k_{eff} \to k_b$; i.e., the stiffness of the interfacial bond dominates the

overall stiffness of the system. In this situation, the cell can hardly sense any changes in substrate stiffness. A similar idea was adopted by Marcq and colleagues (92) in a 1D model.

These results shed light on a long pursued and debated and frequently asked question—that is, whether cells sense force or deformation in their microenvironment. Saez et al. (121) have shown that the traction forces of epithelial cells are linearly proportional to the rigidity of the substrate, suggesting that cellular forces are regulated by the deformation of the matrix in trying to maintain a homeostatic strain. However, measurements by Freyman et al. (48, 123a) have shown that cell traction is limited by the force rather than the displacement of the medium. This puzzle suggests that there is not a simple monotonic relationship between cell traction and substrate stiffness. The contracting-disk model of He et al. (66) provided a feasible explanation for this apparent paradox in that cells appear to maintain constant strain on soft substrates and constant traction on stiff substrates.

How far can cells feel? This is a central question in cell mechanosensing that can be understood by studying the cell-induced deformation and stress fields of the substrate. He et al. (66) showed that both displacement and stress fields in the substrate decay exponentially according to their depth and distance from the adhering cell, with a characteristic decay length on the same order as that of the cell radius (**Figure 8*c,d***). That is, cell-induced displacement and stress fields in the substrate essentially vanish beyond a critical depth or distance that is comparable to the cell's size, which is consistent with experimental observations (95). This behavior is related to the question of how far cells feel into their microenvironment (130). The decay length is thus defined as the mechanosensing length of the cell. It also has been shown that the mechanosensing length is not sensitive to substrate stiffness for a wide range of stiffnesses.

The concept of mechanosensing length provides useful insights into the mechanisms that bone cells use to sense mechanical signals associated with bone remodeling: Osteoblasts and osteoclasts are normally at the surface of the bone, but osteocytes are embedded in the bone matrix. In this scenario, it is important to know how far the cells can sense mechanical stimuli (141, 142). In the literature on bone remodeling (119), the mechanosensing length is often chosen to be 100 μm, which is consistent with the predictions made by He et al. (66).

Mechanosensing length, as described above, also has important implications for the experimental measurement of cell-traction forces associated with the surface deformation of a substrate with finite thickness. The contracting-disk model suggests that a substrate with a depth that is greater than the cell's radius can be considered to be a semi-infinite substrate (90). Essentially, the substrate chosen should be thicker than the mechanosensing length if the traction force is to be determined based on the Boussinesq–Cerruti solution.

What is the role of the cell-shape-dependent distribution of traction in cell migration? This question is important for understanding how cells produce and regulate the driving force for cell migration. Migrating cells normally have a polarized shape (81, 153). For instance, migrating fibroblasts display a large front (lamellipodia) and a long tail. In this specific shape, the area of the cell's front is much larger than the tail, and the cell's center is located closer to the front (35). Correspondingly, polarized keratocytes have a crescent-like shape consisting of a large front and two flank-like rears (18), and the cell's center is also closer to the front. According to the traction–distance relationship predicted from the contracting-disk model, the larger the distance from the cell center, the greater the cell's traction (66). Therefore, traction should be greater at the cell's tail than at the front.

This law of the distribution of traction that is dependent on cell shape is consistent with experimentally measured traction distributions in fibroblasts and keratocytes (18, 35, 47), and it is central to cell migration. At the cell front, relatively low traction is used to promote the formation

of FAs (79), while greater traction at the cell rear induces the disassembly of FAs (78, 79), causing detachment of the cell rear, which produces a driving force for cell migration (155). These results also suggest that cell shape could be employed to control cell motility because different cell shapes induce different distributions of cell traction. For instance, it has been found that the higher a cell's polarity, the higher the driving force produced for cell migration (66, 153, 154, 156), which demonstrates the pivotal role cell shape has in cell migration by regulating the distribution of traction in the cell.

Cell Reorientation Upon Cyclic Stretch

Systematic experiments have shown that upon cyclic stretch, initially randomly oriented cells often reorient themselves perpendicularly to the loading direction (**Figure 9*a***) (73, 100, 143).

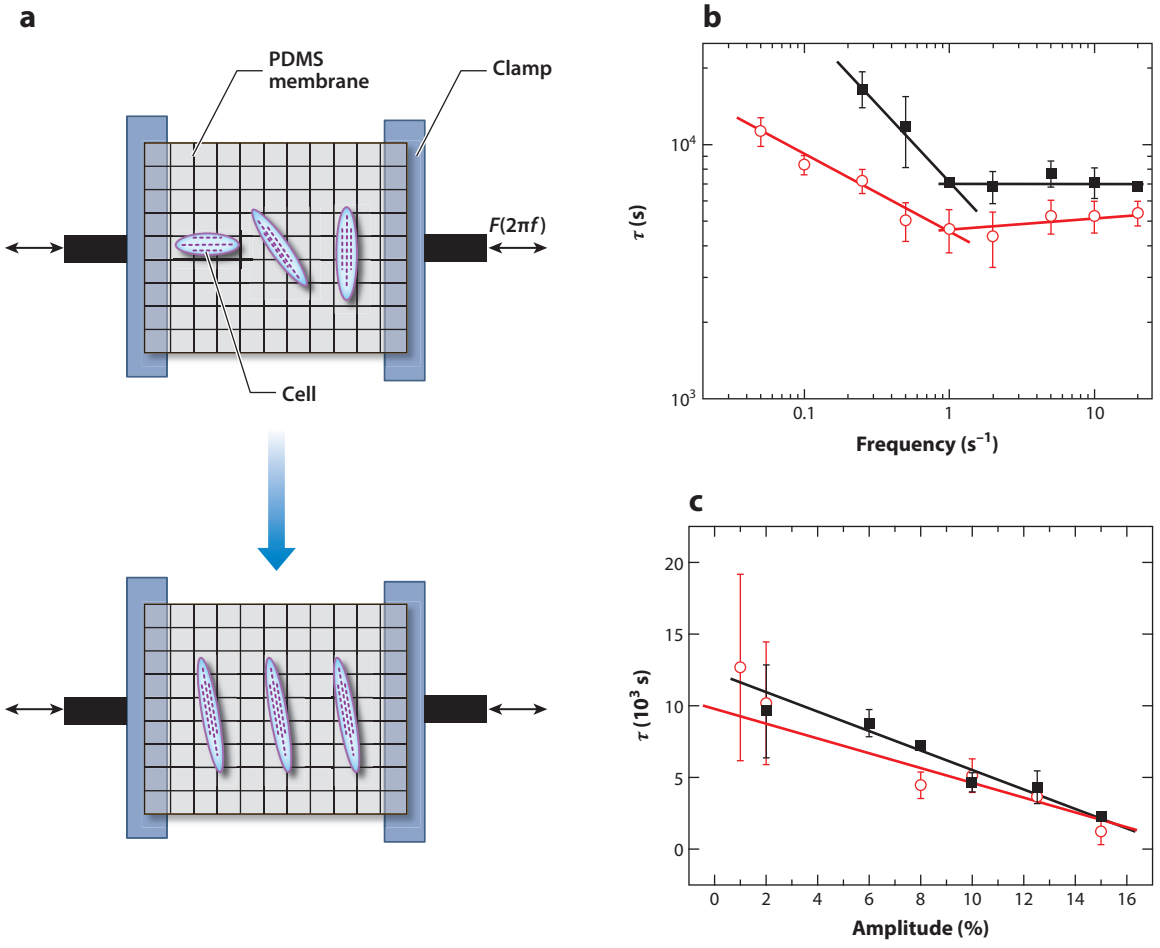

Figure 9

Cell reorientation on an elastic substrate subject to cyclic stretching force, denoted by *F*, with stretching frequency *f*. (*a*) Schematic illustration. (*b*) The characteristic time τ for cell reorientation decreases with cyclic frequency until it saturates beyond 1 Hz for two different cell types under subconfluent conditions. (*c*) The characteristic time τ for cell reorientation decreases linearly with strain amplitude at a cyclic frequency of 1 Hz. Figure adapted from Reference 73 with permission. Abbreviation: PDMS, polydimethylsiloxane.

The duration of the reorientation process strongly depends on both the cycling frequency and amplitude. For cells at subconfluent densities, there exists a lower threshold frequency below which the reorientation process ceases to occur. As the cycling frequency increases, the characteristic time of reorientation decreases monotonically until it saturates at a minimum value beyond 1 Hz (73) (**Figure 9*b***). The characteristic time of reorientation also decreases monotonically with the cycling amplitude (**Figure 9*c***).

A phenomenological model of a force dipole has suggested that the nearly perpendicular reorientation of SFs is caused by a cell's inherent tendency to establish an optimal internal stress (31). However, the same model also predicted that cells should align in parallel with the stretch direction at the limit of very low frequencies, which appears to be inconsistent with experimental observations (73). When considering the effect of cyclic loads on SFs (75, 78), it has been shown that SFs behave elastically at high stretch frequencies, but can adjust their reference lengths at low frequencies to maintain tensional homeostasis (16, 97). Thus, cell reorientation can be viewed as a consequence of the disassembly of SFs under high cyclic frequencies together with a gradual accumulation of SFs in orientations that avoid rapid length changes (75, 157).

Since FAs are one of the key players in cellular reorientation under cyclic stretch (61), an elastosarcomere-adhesion (ELSA) model (schematically shown in **Figure 10*a***) has been developed to integrate the dynamic behaviors of an SF adhering on a substrate via two FAs (24). This model has also incorporated the experimental observations that $\alpha_5\beta_1$ integrin, which is a catch bond (80), plays a dominant role in determining the mechanical strength of FAs (117). Interestingly, the effect of force on the stability of catch bonds is similar to the mechanosensitivity of FAs; i.e., a small force promotes stability and growth, but a large force induces instability. The ELSA model postulates that FAs are catch-bond clusters, and the force in each catch bond is initially close to the optimal value corresponding to the longest lifetime at which FAs are expected to be most stable. SFs were assumed to actively resist stretching, according to the linear Hill's law. However, the

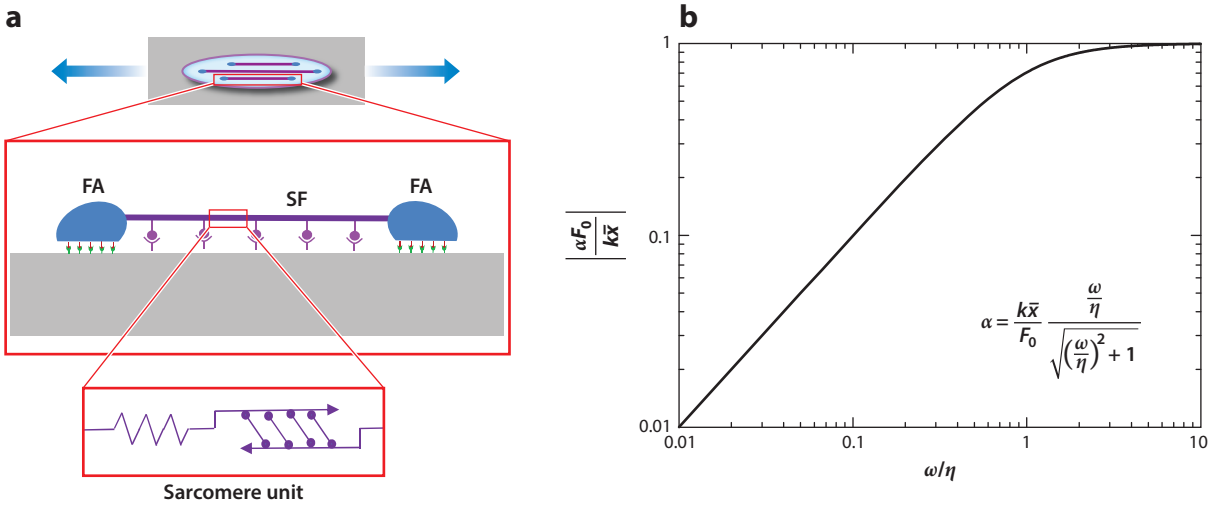

Figure 10

An elastosarcomere-adhesion (ELSA) model of cellular response on a cyclically stretched substrate. (*a*) Schematic illustration of the model. (*b*) The predicted amplitude of steady-state force oscillation in a homogeneously activated stress fiber (SF) as a function of the stretching frequency, f. Note that $\omega = 2\pi f$, k is the spring constant of a sarcomere unit, F_0 is the isometric load, $\bar{x}$ is the stretching amplitude, and η is the characteristic frequency of an SF. Figure adapted from Reference 24 with permission. Abbreviation: FA, focal adhesion.

shortening or lengthening of an SF can be nonuniform along its length (107, 134). In the ELSA model, two activation modes of SF contraction were assumed. In the localized activation mode, only one or a few sarcomere units in an SF are activated at any given time, but in the homogeneous activation mode, all or a large majority of sarcomere units are simultaneously activated (24). As schematically shown in **Figure 10*a***, it has been suggested that there are multiple localized anchor points along an SF (64), and these are expected to have intrinsic relaxation timescales that are much shorter than those of mature FAs. At low stretch frequencies, the interaction forces between the SF and the substrate via the localized anchor points may be fully relaxed due to bond rupturing and rebinding. However, at high frequencies, there may not be sufficient time for these bonds to relax, and the whole SF would then be stretched directly by the substrate via these anchoring points, which would lead to homogeneous activation of all or a majority of the sarcomere units (24).

The ELSA model also predicted that the force within the SF oscillates around the isometric load upon cyclic stretch, with the amplitude increasing with that of the cyclic strain and also with the stretch frequency until it saturates beyond a critical frequency (**Figure 10*b***). The saturation frequency was predicted to be controlled by two intrinsic clocks in the SF (24). The upper intrinsic clock corresponds to the characteristic frequency associated with the homogeneous activation mode of an SF:

$$f_{\mathrm{h}} = \frac{kV_0}{2\pi F_0}, \qquad 13a.$$

where $k \sim 1$ pN/nm is the spring constant of the SF; the lower intrinsic clock corresponds to the characteristic frequency associated with the homogeneous activation mode of an SF:

$$f_{\mathrm{l}} = \frac{kV_0}{2N\pi F_0}, \qquad 13b.$$

where N is the total number of sarcomere units in an SF along its length. It was estimated that $f_{\mathrm{l}} \sim 0.002$–$0.02$ Hz, and $f_{\mathrm{h}} \sim 0.12$–1.2 Hz (24). The observed threshold frequencies for cell reorientation are 0.01 Hz for rat fibroblasts and 0.1 Hz for human fibroblasts (73), which are close to f_{l}, suggesting that the localized activation mode of SFs may govern reorientation behavior in the low-frequency regime. In contrast, f_{h} is close to the experimentally reported saturation frequency, around 1 Hz, and beyond which the characteristic time of cell reorientation no longer changes (73). This is consistent with the assumption that the homogeneous activation mode of SFs governs reorientation behavior in the high-frequency regime (24).

The ELSA model also predicted that FAs essentially maintain their sizes upon cyclic stretch due to the much longer characteristic timescale associated with FA growth or shrinkage (24), which is consistent with the observation that massive FA rearrangements under cyclic stretch are accomplished by sliding instead of de novo formation of FAs during the initial process (61). As the force in the catch bonds oscillates periodically about the optimal load, the bond lifetime was predicted to decrease with cycling frequency until it reached approximately 1 Hz, beyond which it saturates to a constant (24). The bond lifetime also has been shown to decrease monotonically with cycling amplitude. These results are qualitatively consistent with the reported behaviors of the characteristic time it takes for cell reorientation (73). The ELSA model also predicted that SFs would favor an orientation nearly perpendicular to the stretch direction, where the minimum stretch amplitude exists. With less stable FAs postulated to slide or relocate to more stable configurations, the rotation velocity was estimated using a simple transition-state model (24).

Experiments have shown that stretching affects the reorientation of stress fibers more significantly than does relaxation (139). To understand this effect, it had been assumed that in the vicinity of the isometric force the shortening speed of an SF is higher than its lengthening speed (24), similar to the behavior of skeletal muscle (22). The effect of cyclic stretch with

triangular waveforms was then investigated, and this showed that applying a high lengthening rate leads to much larger forces within SFs than applying a fast shortening rate (24). This implies that, at the same strain rate, lengthening should be more effective in destabilizing catch bonds, and this explains the observed asymmetric effect that SFs are more responsive to lengthening than to shortening (139). The ELSA model cautioned that there could be alternative physical interpretations for the catch-bond-like behaviors of FAs.

Zhong et al. (157) also predicted the biphasically frequency-dependent cell reorientation by modeling the disassembly of original SFs along the stretching direction as well as the formation of new SFs perpendicular to the loading direction. More recently, Qian et al. (111) developed another promising model of cyclic stretch-induced reorientation of spindle-shaped cells from the point of view of competitive coupling between the assembly and disassembly of SFs, the growth and disruption of FAs, the stiffening of the substrate during stretch, and rotation of the whole cell. The hypothesis that cells tend to orient in the direction where the formation of SFs is energetically most favorable suggests that the final alignment of cells reflects the competition between the elevated force within SFs that accelerates their disassembly and the disruption of cell–substrate adhesion, and an effectively increased substrate rigidity that promotes more stable FAs. The model integrates observations about the dependence of stable adhesions on substrate rigidity and the dependence of cell realignment on stretching frequency and amplitude, and also provides a simple explanation of the regulation of the protein Rho in the formation of stretch-induced SFs in cells.

FUTURE CHALLENGES

Understanding the mechanics of active mechanosensing by cells is a multiscale problem that is full of challenges and opportunities. A cell is a complex, multiscale living system with a myriad of functions and processes occurring from the molecular to the subcellular and cellular levels. At the level of FAs and SFs, there exist all kinds of interactions among numerous proteins in the mechanosensing of cells. The nanoscale architecture of FAs has been identified using interferometric photoactivated localization microscopy (74). This revealed that integrins and actin are vertically separated by a 40 nm FA core region, consisting of multiple protein-specific layers, including an integrin-signaling layer, an intermediate-force transduction layer, and an uppermost actin-regulatory layer. There are also complex interactions at the subcellular level, including those among sarcomere-like units of SFs and their connected cell–matrix adhesive structures. Cell adhesion, cell migration, and other adhesion-related behaviors all require coordination among multiple cell–matrix adhesion sites. There also exists crosstalk between cell–ECM and cell–cell contacts (94). Collective cell migration requires coordination among FAs in different cells. In addition, the actin–myosin contractility in striated fibers close to the basal membrane induces substrate strain that gives rise to an elastic interaction between neighboring striated fibers, which in turn favors interfiber registry and predicts the dependence of interfiber registry on externally controllable elastic properties in the substrate. Modeling such a complex system is challenging. It will be desirable to identify a minimal modeling system for each length scale.

The timescale and its interplay with the length scale are also important issues in the mechanosensing of cells. Clearly, events involved in the active mechanosensing of cells often occur at multiple timescales. Ion channel protein is activated as quickly as 0.1 s (77); the association or dissociation of a molecular complex can happen within seconds; the assembly of mature FAs takes approximately 3 minutes; and gene regulation in stem-cell differentiation can take up to a few days. Correspondingly, the size of a single protein at a specific state with a particular structure is approximately 10 nm; the size of an FA is approximately 1 μm; and the length of an SF or the size of a cell is approximately 50 μm. Consequently, the events that take place in

cell–matrix adhesion at any of those timescales or length scales may be critical, especially when their effects are highly magnified through multiple rounds of mechanosensing at multiple sites. Thus, it is important to first identify all these events at different timescales and length scales, and then provide an integrated hierarchical modeling system to quantitatively evaluate the contributions of these events in the active cell–matrix adhesion.

In moving toward an integrated approach, there is a compelling need to integrate different subcellular components with sufficient structural details at the molecular level to elucidate specific functions and behaviors at the higher structural levels of cells (65) with the aim of establishing a comprehensive theoretical framework to understand and guide mounting experimental observations. One example would be to study the underlying mechanisms that control the magnitude of pre-strain in living systems at different length scales: For instance, pre-strain in stress fibers is 0.1–0.2, and at the cellular level is approximately 0.1, according to experimental findings (32, 87). There even exist homeostatic eigenstrains at the scale of tissue such as bone, tendon, or blood vessel (2, 7, 63). However, the underlying mechanisms—which seem to involve many length scales, from molecular to subcellular to cellular—that determine the value of the eigenstrains in cells and tissues remain to be fully clarified. Another example is the biphasic dependence of cell sensing on substrate stiffness at both the cellular and molecular levels. It will be interesting to find the connections among stiffness sensing at different length scales.

CONCLUSIONS

In this article we have reviewed some recent modeling studies of active mechanosensing in cell–matrix interactions at different length scales. It is clear that cells can sense mechanical cues at different length scales through different responding mechanisms. The mechanosensing structures involved include receptor–ligand bonds at the molecular level, FA complex and associated SFs at the subcellular level, and the overall structure and alignment of the cytoskeleton, as well as contractile deformation and associated cell traction at the cellular level.

The mechanical cues, including rigidity, morphology, and deformation of the matrix, as well as internal and external forces, play critical parts in regulating the mechanosensing of cells. The influence of the mechanical cues will either propagate from the molecular scale to the cellular scale via force transduction, or propagate down to the molecular scale. For instance, on one hand, micropatterns and the stiffness of the ECM will influence the distribution of traction force at the cellular scale, which then locally (at the subcellular level) influences the stability of FAs, such as the formation at cell front and de-adhesion at cell rear. At the molecular level, the traction force can influence the binding and unbinding dynamics of receptor–ligand bonds in FAs. On the other hand, substrate stiffness not only influences the deformation and traction of cells at the cellular scale, but also directly influences the stability of FAs (bond clusters), as well as the binding and unbinding of bonds at the molecular level.

It has been observed that there exist intrinsic biphasic features in the mechanosensing behaviors of cells. These biphasic behaviors can happen at different length scales. Cells do not have simple monotonic responses to an external stimulus. For example, at the cellular level, the magnitude of cell traction depends biphasically on matrix stiffness. At the subcellular level, the stability of FAs depends biphasically on the magnitude of the traction force. At the molecular level, the bond-rupture force depends biphasically on the loading stiffness and loading rate.

There are intrinsic and internal relationships among the different mechanisms of mechanosensing behaviors. For example, in the mechanisms of cells regulating cell–matrix adhesion, the cellular-level traction–distance relationship combined with the subcellular-level biphasic dependence of the stability of FAs on the traction force forms the basis of cells regulating their migration

behaviors. This mechanism allows cells to form adhesion (FA complexes) at the cell front and to detach at the cell rear.

We have also discussed some interesting size effects in cellular mechanosensing. For example, the size of a molecular cluster has a crucial role in the adhesion strength of FAs; cell size influences the magnitude of cell traction (the larger the cell size or the larger the distance from the cell center, the stronger the traction); and mechanosensing length depends on cell size. The timescale also matters. For example, the loading frequency has important roles in cell reorientation: At a sufficiently low loading frequency, cells barely change their orientation, but at a higher loading frequency, cells reorient themselves to align perpendicularly to the loading direction. Bond rupture also depends on the loading rate: When the loading rate is high, the rupture strength decreases with the loading rate, but when the loading rate decreases to a critical loading rate, the rupture force will level off to a saturation value that is independent of the loading rate.

SUMMARY POINTS

1. Mechanosensing events take place at the single-molecule level with the aid of mechanical forces induced by myosin motors in stress fibers.
2. The interaction among proteins is mediated by weak but specific binding. Three types of bonds have been reported: ideal bonds, slip bonds, and catch bonds. The loading rate, loading magnitude, and elasticity have a strong effect on the binding kinetics among proteins.
3. Focal adhesions are mechanosensitive and also heterogeneous in many aspects.
4. A cluster of bonds has a much longer lifetime than a single bond due to cooperative binding within a confined environment; however, this is influenced by the elasticity of the substrate, bond spacing, and pre-tension within the cytoskeleton.
5. A coupled stochastic–elastic framework can be adapted to build a molecular model to study the mechanical behavior of stress fibers.
6. Cell traction generally increases as distance from the cell center increases. This law of traction–distance distribution suggests that cell shape (polarization) has an important role in regulating the speed and direction of cell migration.
7. Cell traction exhibits a biphasic dependence on substrate stiffness: It increases as the stiffness of a soft substrate increases (corresponding to a constant deformation or strain), and then levels off to a constant value on a stiff substrate.
8. Cells rotate upon cyclic stretch. Both the cycling frequency and the amplitude regulate the duration of the cell-reorientation process.

FUTURE ISSUES

1. What is the complete list of mechanosensing events at the molecular level?
2. How does the loading rate of focal adhesions that is due to sarcomere contraction depend on matrix rigidity?

3. How is a stress fiber assembled?
4. What are the potential roles of catch bonds in the dynamics of focal adhesion and in the regulation of cell migration?
5. How does matrix rigidity regulate gene expression?
6. Which level of rigidity does a cell sense on a highly heterogeneous matrix?
7. Is there any physical connection between stress fibers and the matrix beyond the two ends?
8. How does a stress fiber shorten or lengthen upon cyclic stretch?
9. How does a focal adhesion remodel under cyclic stretch?
10. How does a cell distinguish between 2D and 3D environments?

DISCLOSURE STATEMENT

The authors are not aware of any affiliations, memberships, funding, or financial holdings that might be perceived as affecting the objectivity of this review.

ACKNOWLEDGMENTS

This work was supported by the National Natural Science Foundation of China (grant nos. 11372279, 11321202, 11372042, and 11221202) and Fundamental Research Funds for the Central Universities (no. 2013QNA4045). The work of H.G. has been supported by the US National Science Foundation (grant no. CMMI-1028530) and the Center for Mechanics and Materials at Tsinghua University.

LITERATURE CITED

1. Alexandrova AY, Arnold K, Schaub S, Vasiliev JM, Meister J-J, et al. 2008. Comparative dynamics of retrograde actin flow and focal adhesions: Formation of nascent adhesions triggers transition from fast to slow flow. *PLOS ONE* 3:e3234
2. Arampatzis A, Karamanidis K, Albracht K. 2007. Adaptational responses of the human Achilles tendon by modulation of the applied cyclic strain magnitude. *J. Exp. Biol.* 210:2743–53
3. Arnold M, Cavalcanti-Adam EA, Glass R, Blummel J, Eck W, et al. 2004. Activation of integrin function by nanopatterned adhesive interfaces. *ChemPhysChem* 5:383–88
4. Arnold M, Hirschfeld-Warneken VC, Lohmuller T, Heil P, Blummel J, et al. 2008. Induction of cell polarization and migration by a gradient of nanoscale variations in adhesive ligand spacing. *Nano Lett.* 8:2063–69
5. Ayala I, Baldassarre M, Caldieri G, Buccione R. 2006. Invadopodia: a guided tour. *Eur. J. Cell Biol.* 85:159–64
6. Balaban NQ, Schwarz US, Riveline D, Goichberg P, Tzur G, et al. 2001. Force and focal adhesion assembly: a close relationship studied using elastic micropatterned substrates. *Nat. Cell Biol.* 3:466–72
7. Bayraktar HH, Keaveny TM. 2004. Mechanisms of uniformity of yield strains for trabecular bone. *J. Biomech.* 37:1671–78
8. Bell GI. 1978. Models for the specific adhesion of cells to cells. *Science* 200:618–27
9. Bershadsky AD, Balaban NQ, Geiger B. 2003. Adhesion-dependent cell mechanosensitivity. *Annu. Rev. Cell Dev. Biol.* 19:677–95

10. Bershadsky AD, Tint IS, Neyfakh AA, Vasiliev JM. 1985. Focal contacts of normal and RSV-transformed quail cells. Hypothesis of the transformation-induced deficient maturation of focal contacts. *Exp. Cell Res.* 158:433–44
11. Besser A, Colombelli J, Stelzer EHK, Schwarz US. 2011. Viscoelastic response of contractile filament bundles. *Phys. Rev. E* 83:051902
12. Besser A, Schwarz US. 2007. Coupling biochemistry and mechanics in cell adhesion: a model for inhomogeneous stress fiber contraction. *New J. Phys.* 9:425
13. Bihr T, Seifert U, Smith A-S. 2012. Nucleation of ligand-receptor domains in membrane adhesion. *Phys. Rev. Lett.* 109:258101
14. Boal D. 2002. *Mechanics of the Cell*. Cambridge, UK: Cambridge Univ. Press
15. Brown NH, Gregory SL, Rickoll WL, Fessler LI, Prout M, et al. 2002. Talin is essential for integrin function in *Drosophila*. *Dev. Cell* 3:569–79
16. Brown RA, Prajapati R, McGrouther DA, Yannas IV, Eastwood M. 1998. Tensional homeostasis in dermal fibroblasts: mechanical responses to mechanical loading in three-dimensional substrates. *J. Cell. Physiol.* 175:323–32
17. Burridge K, Chrzanowska-Wodnicka M. 1996. Focal adhesions, contractility, and signaling. *Annu. Rev. Cell Dev. Biol.* 12:463–519
18. Burton K, Park JH, Taylor DL. 1999. Keratocytes generate traction forces in two phases. *Mol. Biol. Cell* 10:3745–69
19. Byron A, Morgan MR, Humphries MJ. 2010. Adhesion signalling complexes. *Curr. Biol.* 20:R1063–67
20. Chan CE, Odde DJ. 2008. Traction dynamics of filopodia on compliant substrates. *Science* 322:1687–91
21. Chen B. 2013. Self-regulation of motor force through chemomechanical coupling in skeletal muscle contraction. *J. Appl. Mech.* 80:051013
22. Chen B, Gao H. 2011. Motor force homeostasis in skeletal muscle contraction. *Biophys. J.* 101:396–403
23. Chen B, Gao HJ. 2010. Mechanical principle of enhancing cell-substrate adhesion via pre-tension in the cytoskeleton. *Biophys. J.* 98:2154–62
24. Chen B, Kemkemer R, Deibler M, Spatz J, Gao H. 2012. Cyclic stretch induces cell reorientation on substrates by destabilizing catch bonds in focal adhesions. *PLOS ONE* 7:e48346
25. Choi CK, Vicente-Manzanares M, Zareno J, Whitmore LA, Mogilner A, Horwitz AR. 2008. Actin and α-actinin orchestrate the assembly and maturation of nascent adhesions in a myosin II motor-independent manner. *Nat. Cell Biol.* 10:1039–50
26. Clark K, Pankov R, Travis MA, Askari JA, Mould AP, et al. 2005. A specific $\alpha_5\beta_1$-integrin conformation promotes directional integrin translocation and fibronectin matrix formation. *J. Cell Sci.* 118:291–300
27. Colombelli J, Besser A, Kress H, Reynaud EG, Girard P, et al. 2009. Mechanosensing in actin stress fibers revealed by a close correlation between force and protein localization. *J. Cell Sci.* 122:1665–79
28. Cooke R. 1986. The mechanism of muscle contraction. *CRC Crit. Rev. Biochem.* 21:53–118
29. Costa KD, Hucker WJ, Yin FCP. 2002. Buckling of actin stress fibers: a new wrinkle in the cytoskeletal tapestry. *Cell Motil. Cytoskelet.* 52:266–74
30. Curtis AS. 1964. The mechanism of adhesion of cells to glass. A study by interference reflection microscopy. *J. Cell Biol.* 20:199–215
31. De R, Zemel A, Safran SA. 2007. Dynamics of cell orientation. *Nat. Phys.* 3:655–59
32. Deguchi S, Ohashi T, Sato M. 2006. Tensile properties of single stress fibers isolated from cultured vascular smooth muscle cells. *J. Biomech.* 39:2603–10
33. del Rio A, Perez-Jimenez R, Liu R, Roca-Cusachs P, Fernandez JM, Sheetz MP. 2009. Stretching single talin rod molecules activates vinculin binding. *Science* 323:638–41
34. Dembo M, Torney DC, Saxman K, Hammer D. 1988. The reaction-limited kinetics of membrane-to-surface adhesion and detachment. *Proc. R. Soc. Lond. B* 234:55–83
35. Dembo M, Wang Y-L. 1999. Stresses at the cell-to-substrate interface during locomotion of fibroblasts. *Biophys. J.* 76:2307–16

36. Endlich N, Otey CA, Kriz W, Endlich K. 2007. Movement of stress fibers away from focal adhesions identifies focal adhesions as sites of stress fiber assembly in stationary cells. *Cell Motil. Cytoskelet.* 64:966–76
37. Engler AJ, Sen S, Sweeney HL, Discher DE. 2006. Matrix elasticity directs stem cell lineage specification. *Cell* 126:677–89
38. Erdmann T, Schwarz US. 2004. Stability of adhesion clusters under constant force. *Phys. Rev. Lett.* 92:108102
39. Erdmann T, Schwarz US. 2004. Stochastic dynamics of adhesion clusters under shared constant force and with rebinding. *J. Chem. Phys.* 121:8997–9017
40. Erdmann T, Schwarz US. 2006. Bistability of cell-matrix adhesions resulting from non-linear receptor-ligand dynamics. *Biophys. J.* 91:L60–62
41. Erdmann T, Schwarz US. 2007. Impact of receptor-ligand distance on adhesion cluster stability. *Eur. Phys. J. E* 22:123–37
42. Evans E. 2001. Probing the relation between force—lifetime—and chemistry in single molecular bonds. *Annu. Rev. Biophys. Biomol. Struct.* 30:105–28
43. Evans E, Leung A, Heinrich V, Zhu C. 2004. Mechanical switching and coupling between two dissociation pathways in a P-selectin adhesion bond. *PNAS* 101:11281–86
44. Evans E, Ludwig F. 2000. Dynamic strengths of molecular anchoring and material cohesion in fluid biomembranes. *J. Phys. Condens. Matter* 12:A315
45. Evans E, Ritchie K. 1997. Dynamic strength of molecular adhesion bonds. *Biophys. J.* 72:1541–55
46. Evans EA, Calderwood DA. 2007. Forces and bond dynamics in cell adhesion. *Science* 316:1148–53
47. Fournier MF, Sauser R, Ambrosi D, Meister J-J, Verkhovsky AB. 2010. Force transmission in migrating cells. *J. Cell Biol.* 188:287–97
48. Freyman TM, Yannas IV, Yokoo R, Gibson LJ. 2002. Fibroblast contractile force is independent of the stiffness which resists the contraction. *Exp. Cell Res.* 272:153–62
49. Fu J, Wang Y-K, Yang MT, Desai RA, Yu X, et al. 2010. Mechanical regulation of cell function with geometrically modulated elastomeric substrates. *Nat. Methods* 7:733–36
50. Gao H, Qian J, Chen B. 2011. Probing mechanical principles of focal contacts in cell-matrix adhesion with a coupled stochastic-elastic modelling framework. *J. R. Soc. Interface* 8:1217–32
51. Gardel ML, Sabass B, Ji L, Danuser G, Schwarz US, Waterman CM. 2008. Traction stress in focal adhesions correlates biphasically with actin retrograde flow speed. *J. Cell Biol.* 183:999–1005
52. Geeves MA, Holmes KC. 1999. Structural mechanism of muscle contraction. *Annu. Rev. Biochem.* 68:687–728
53. Geiger B, Bershadsky A. 2001. Assembly and mechanosensory function of focal contacts. *Curr. Opin. Cell Biol.* 13:584–92
54. Geiger B, Bershadsky A, Pankov R, Yamada KM. 2001. Transmembrane extracellular matrix-cytoskeleton crosstalk. *Nat. Rev. Mol. Cell Biol.* 2:793–805
55. Geiger B, Spatz JP, Bershadsky AD. 2009. Environmental sensing through focal adhesions. *Nat. Rev. Microbiol.* 10:21–33
56. Georges PC, Janmey PA. 2005. Cell type-specific response to growth on soft materials. *J. Appl. Physiol.* 98:1547–53
57. Ghibaudo M, Saez A, Trichet L, Xayaphoummine A, Browaeys J, et al. 2008. Traction forces and rigidity sensing regulate cell functions. *Soft Matter* 4:1836–43
58. Gilmore AP, Burridge K. 1996. Molecular mechanisms for focal adhesion assembly through regulation of protein–protein interactions. *Structure* 4:647–51
59. Gimona M, Buccione R. 2006. Adhesions that mediate invasion. *Int. J. Biochem. Cell Biol.* 38:1875–92
60. Gingras AR, Ziegler WH, Frank R, Barsukov IL, Roberts GCK, et al. 2005. Mapping and consensus sequence identification for multiple vinculin binding sites within the talin rod. *J. Biol. Chem.* 280:37217–24
61. Goldyn AM, Rioja BA, Spatz JP, Ballestrem C, Kemkemer R. 2009. Force-induced cell polarisation is linked to RhoA-driven microtubule-independent focal-adhesion sliding. *J. Cell Sci.* 122:3644–51
62. Guo B, Guilford WH. 2006. Mechanics of actomyosin bonds in different nucleotide states are tuned to muscle contraction. *PNAS* 103:9844–49

63. Guo X, Lu X, Kassab GS. 2005. Transmural strain distribution in the blood vessel wall. *Am. J. Physiol. Heart Circ. Physiol.* 288:H881–86
64. Guthardt Torres P, Bischofs IB, Schwarz US. 2012. Contractile network models for adherent cells. *Phys. Rev. E* 85:011913
65. Hanein D, Horwitz AR. 2012. The structure of cell-matrix adhesions: the new frontier. *Curr. Opin. Cell Biol.* 24:134–40
66. He S, Su Y, Ji B, Gao H. 2014. Some basic questions on mechanosensing in cell–substrate interaction. *J. Mech. Phys. Solids* 70:116–35
67. Heath JP, Dunn GA. 1978. Cell to substratum contacts of chick fibroblasts and their relation to the microfilament system. A correlated interference-reflexion and high-voltage electron-microscope study. *J. Cell Sci.* 29:197–212
68. Hill TL. 1987. *Linear Aggregation Theory in Cell Biology*. New York: Springer-Verlag
69. Hotulainen P, Lappalainen P. 2006. Stress fibers are generated by two distinct actin assembly mechanisms in motile cells. *J. Cell Biol.* 173:383–94
70. Huang B, Babcock H, Zhuang X. 2010. Breaking the diffraction barrier: super-resolution imaging of cells. *Cell* 143:1047–58
70a. Hytönen VP, Vogel V. 2008. How force might activate talin's vinculin binding sites: SMD reveals a structural mechanism. *PLOS Comput. Biol.* 4:e24
71. Ji B, Bao G. 2011. Cell and molecular biomechanics: perspectives and challenges. *Acta Mech. Solida Sin.* 24:27–51
72. Jiang G, Giannone G, Critchley DR, Fukumoto E, Sheetz MP. 2003. Two-piconewton slip bond between fibronectin and the cytoskeleton depends on talin. *Nature* 424:334–37
73. Jungbauer S, Gao H, Spatz JP, Kemkemer R. 2008. Two characteristic regimes in frequency-dependent dynamic reorientation of fibroblasts on cyclically stretched substrates. *Biophys. J.* 95:3470–78
74. Kanchanawong P, Shtengel G, Pasapera AM, Ramko EB, Davidson MW, et al. 2010. Nanoscale architecture of integrin-based cell adhesions. *Nature* 468:580–84
75. Kaunas R, Hsu H-J, Deguchi S. 2011. Sarcomeric model of stretch-induced stress fiber reorganization. *Cell Health Cytoskelet.* 3:13–22
76. Kaverina I, Krylyshkina O, Beningo K, Anderson K, Wang Y-L, Small JV. 2002. Tensile stress stimulates microtubule outgrowth in living cells. *J. Cell Sci.* 115:2283–91
77. Kobayashi T, Sokabe M. 2010. Sensing substrate rigidity by mechanosensitive ion channels with stress fibers and focal adhesions. *Curr. Opin. Cell Biol.* 22:669–76
78. Kong D, Ji B, Dai L. 2008. Stability of adhesion clusters and cell reorientation under lateral cyclic tension. *Biophys. J.* 95:4034–44
79. Kong D, Ji B, Dai L. 2010. Stabilizing to disruptive transition of focal adhesion response to mechanical forces. *J. Biomech.* 43:2524–29
80. Kong F, García AJ, Mould AP, Humphries MJ, Zhu C. 2009. Demonstration of catch bonds between an integrin and its ligand. *J. Cell Biol.* 185:1275–84
81. Kozlov MM, Mogilner A. 2007. Model of polarization and bistability of cell fragments. *Biophys. J.* 93:3811–19
82. Kumar S, Maxwell IZ, Heisterkamp A, Polte TR, Lele TP, et al. 2006. Viscoelastic retraction of single living stress fibers and its impact on cell shape, cytoskeletal organization, and extracellular matrix mechanics. *Biophys. J.* 90:3762–73
83. Lecuit T, Lenne P-F. 2007. Cell surface mechanics and the control of cell shape, tissue patterns and morphogenesis. *Nat. Rev. Microbiol.* 8:633–44
83a. Legant WR, Choi CK, Miller JS, Shao L, Gao L, et al. 2013. Multidimensional traction force microscopy reveals out-of-plane rotational moments about focal adhesions. *PNAS* 110:881–86
84. Legant WR, Miller JS, Blakely BL, Cohen DM, Genin GM, Chen CS. 2010. Measurement of mechanical tractions exerted by cells in three-dimensional matrices. *Nat. Methods* 7:969–71
85. Li D, Ji B. 2014. Predicted rupture force of a single molecular bond becomes rate independent at ultralow loading rates. *Phys. Rev. Lett.* 112:078302
86. Lo C-M, Wang H-B, Dembo M, Wang Y-l. 2000. Cell movement is guided by the rigidity of the substrate. *Biophys. J.* 79:144–52

87. Lu L, Feng Y, Hucker WJ, Oswald SJ, Longmore GD, Yin FCP. 2008. Actin stress fiber pre-extension in human aortic endothelial cells. *Cell Motil. Cytoskelet.* 65:281–94
88. Luo B-H, Carman CV, Springer TA. 2007. Structural basis of integrin regulation and signaling. *Annu. Rev. Immunol.* 25:619–47
89. Lymn RW, Taylor EW. 1971. Mechanism of adenosine triphosphate hydrolysis by actomyosin. *Biochemistry* 10:4617–24
90. Maloney J, Walton E, Bruce C, Van Vliet K. 2008. Influence of finite thickness and stiffness on cellular adhesion-induced deformation of compliant substrata. *Phys. Rev. E* 78:041923
91. Mao Y, Schwarzbauer JE. 2005. Fibronectin fibrillogenesis, a cell-mediated matrix assembly process. *Matrix Biol.* 24:389–99
92. Marcq P, Yoshinaga N, Prost J. 2011. Rigidity sensing explained by active matter theory. *Biophys. J.* 101:L33–35
93. Marshall BT, Long M, Piper JW, Yago T, McEver RP, Zhu C. 2003. Direct observation of catch bonds involving cell-adhesion molecules. *Nature* 423:190–93
94. Maruthamuthu V, Sabass B, Schwarz US, Gardel ML. 2011. Cell-ECM traction force modulates endogenous tension at cell–cell contacts. *PNAS* 108:4708–13
94a. Maskarinec SA, Franck C, Tirrell DA, Ravichandran G. 2009. Quantifying cellular traction forces in three dimensions. *PNAS* 106:22108–13
95. Merkel R, Kirchgessner N, Cesa CM, Hoffmann B. 2007. Cell force microscopy on elastic layers of finite thickness. *Biophys. J.* 93:3314–23
96. Mertz A, Banerjee S, Che Y, German G, Xu Y, et al. 2012. Scaling of traction forces with the size of cohesive cell colonies. *Phys. Rev. Lett.* 108:198101
97. Mizutani T, Haga H, Kawabata K. 2004. Cellular stiffness response to external deformation: tensional homeostasis in a single fibroblast. *Cell Motil. Cytoskelet.* 59:242–48
98. Morgan MR, Humphries MJ, Bass MD. 2007. Synergistic control of cell adhesion by integrins and syndecans. *Nat. Rev. Microbiol.* 8:957–69
99. Naumanen P, Lappalainen P, Hotulainen P. 2008. Mechanisms of actin stress fibre assembly. *J. Microsc.* 231:446–54
100. Neidlinger-Wilke C, Wilke HJ, Claes L. 1994. Cyclic stretching of human osteoblasts affects proliferation and metabolism: a new experimental method and its application. *J. Orthop. Res.* 12:70–78
101. Oakes PW, Beckham Y, Stricker J, Gardel ML. 2012. Tension is required but not sufficient for focal adhesion maturation without a stress fiber template. *J. Cell Biol.* 196:363–74
102. Pankov R, Cukierman E, Katz BZ, Matsumoto K, Lin DC, et al. 2000. Integrin dynamics and matrix assembly: tensin-dependent translocation of $\alpha_5\beta_1$ integrins promotes early fibronectin fibrillogenesis. *J. Cell Biol.* 148:1075–90
103. Paszek MJ, Zahir N, Johnson KR, Lakins JN, Rozenberg GI, et al. 2005. Tensional homeostasis and the malignant phenotype. *Cancer Cell* 8:241–54
104. Pelham RJ, Wang YL. 1997. Cell locomotion and focal adhesions are regulated by substrate flexibility. *PNAS* 94:13661–65
105. Peng X, Huang J, Xiong C, Fang J. 2012. Cell adhesion nucleation regulated by substrate stiffness: a Monte Carlo study. *J. Biomech.* 45:116–22
106. Pereverzev YV, Prezhdo OV, Forero M, Sokurenko EV, Thomas WE. 2005. The two-pathway model for the catch-slip transition in biological adhesion. *Biophys. J.* 89:1446–54
107. Peterson LJ, Rajfur Z, Maddox AS, Freel CD, Chen Y, et al. 2004. Simultaneous stretching and contraction of stress fibers in vivo. *Mol. Biol. Cell* 15:3497–508
108. Pourati J, Maniotis A, Spiegel D, Schaffer JL, Butler JP, et al. 1998. Is cytoskeletal tension a major determinant of cell deformability in adherent endothelial cells? *Am. J. Physiol. Cell Physiol.* 274:C1283–89
109. Puklin-Faucher E, Sheetz MP. 2009. The mechanical integrin cycle. *J. Cell Sci.* 122:179–86
110. Qian J, Gao H. 2010. Soft matrices suppress cooperative behaviors among receptor-ligand bonds in cell adhesion. *PLOS ONE* 5:e12342
111. Qian J, Liu H, Lin Y, Chen W, Gao H. 2013. A mechanochemical model of cell reorientation on substrates under cyclic stretch. *PLOS ONE* 8:e65864

112. Qian J, Wang J, Gao H. 2008. Lifetime and strength of adhesive molecular bond clusters between elastic media. *Langmuir* 24:1262–70
113. Qian J, Wang JZ, Lin Y, Gao HJ. 2009. Lifetime and strength of periodic bond clusters between elastic media under inclined loading. *Biophys. J.* 97:2438–45
114. Rape AD, Guo W-h, Wang Y-l. 2011. The regulation of traction force in relation to cell shape and focal adhesions. *Biomaterials* 32:2043–51
115. Reinhart-King CA, Dembo M, Hammer DA. 2005. The dynamics and mechanics of endothelial cell spreading. *Biophys. J.* 89:676–89
116. Riveline D, Zamir E, Balaban NQ, Schwarz US, Ishizaki T, et al. 2001. Focal contacts as mechanosensors: externally applied local mechanical force induces growth of focal contacts by an mDia1-dependent and ROCK-independent mechanism. *J. Cell Biol.* 153:1175–86
117. Roca-Cusachs P, Gauthier NC, del Rio A, Sheetz MP. 2009. Clustering of $\alpha_5\beta_1$ integrins determines adhesion strength whereas $\alpha_v\beta_3$ and talin enable mechanotransduction. *PNAS* 106:16245–50
118. Rottiers P, Saltel F, Daubon T, Chaigne-Delalande B, Tridon V, et al. 2009. TGFβ-induced endothelial podosomes mediate basement membrane collagen degradation in arterial vessels. *J. Cell Sci.* 122:4311–18
119. Ruimerman R, Hilbers P, van Rietbergen B, Huiskes R. 2005. A theoretical framework for strain-related trabecular bone maintenance and adaptation. *J. Biomech.* 38:931–41
120. Russell RJ, Xia S-L, Dickinson RB, Lele TP. 2009. Sarcomere mechanics in capillary endothelial cells. *Biophys. J.* 97:1578–85
121. Saez A, Buguin A, Silberzan P, Ladoux B. 2005. Is the mechanical activity of epithelial cells controlled by deformations or forces? *Biophys. J.* 89:L52–54
122. Sarangapani KK, Yago T, Klopocki AG, Lawrence MB, Fieger CB, et al. 2004. Low force decelerates L-selectin dissociation from P-selectin glycoprotein ligand-1 and endoglycan. *J. Biol. Chem.* 279:2291–98
123. Sawada Y, Tamada M, Dubin-Thaler BJ, Cherniavskaya O, Sakai R, et al. 2006. Force sensing by mechanical extension of the Src family kinase substrate p130Cas. *Cell* 127:1015–26
123a. Schoen I, Pruitt BL, Vogel V. 2013. The yin-yang of rigidity sensing: how forces and mechanical properties regulate the cellular response to materials. *Annu. Rev. Mater. Res.* 43:589–618
124. Schwartz MA, Chen CS. 2013. Cell biology. Deconstructing dimensionality. *Science* 339:402–4
125. Schwartz MA, Ginsberg MH. 2002. Networks and crosstalk: integrin signalling spreads. *Nat. Cell Biol.* 4:E65–68
126. Schwarz US, Erdmann T, Bischofs IB. 2006. Focal adhesions as mechanosensors: the two-spring model. *BioSystems* 83:225–32
127. Schwarz US, Gardel ML. 2012. United we stand: integrating the actin cytoskeleton and cell-matrix adhesions in cellular mechanotransduction. *J. Cell Sci.* 125:3051–60
128. Seifert U. 2000. Rupture of multiple parallel molecular bonds under dynamic loading. *Phys. Rev. Lett.* 84:2750
129. Selhuber-Unkel C, Erdmann T, López-García M, Kessler H, Schwarz US, Spatz JP. 2010. Cell adhesion strength is controlled by intermolecular spacing of adhesion receptors. *Biophys. J.* 98:543–51
130. Sen S, Engler AJ, Discher DE. 2009. Matrix strains induced by cells: computing how far cells can feel. *Cell. Mol. Bioeng.* 2:39–48
131. Shemesh T, Geiger B, Bershadsky AD, Kozlov MM. 2005. Focal adhesions as mechanosensors: a physical mechanism. *PNAS* 102:12383–88
131a. Shemesh T, Verkhovsky AB, Svitkina TM, Bershadsky AD, Kozlov MM. 2009. Role of focal adhesions and mechanical stresses in the formation and progression of the lamellum interface. *Biophys. J.* 97:1254–64
132. Small JV, Rottner K, Kaverina I. 1999. Functional design in the actin cytoskeleton. *Curr. Opin. Cell Biol.* 11:54–60
133. Smith ML, Gourdon D, Little WC, Kubow KE, Eguiluz RA, et al. 2007. Force-induced unfolding of fibronectin in the extracellular matrix of living cells. *PLOS Biol.* 5:e268
134. Stachowiak MR, O'Shaughnessy B. 2008. Kinetics of stress fibers. *New J. Phys.* 10:025002

135. Tadokoro S, Shattil SJ, Eto K, Tai V, Liddington RC, et al. 2003. Talin binding to integrin β tails: a final common step in integrin activation. *Science* 302:103–6
136. Tan JL, Tien J, Pirone DM, Gray DS, Bhadriraju K, Chen CS. 2003. Cells lying on a bed of microneedles: an approach to isolate mechanical force. *PNAS* 100:1484
137. Tee S-Y, Fu J, Chen CS, Janmey PA. 2011. Cell shape and substrate rigidity both regulate cell stiffness. *Biophys. J.* 100:L25–27
137a. Thomas W, Forero M, Yakovenko O, Nilsson L, Vicini P, et al. 2006. Catch-bond model derived from allostery explains force-activated bacterial adhesion. *Biophys. J.* 90:753–64
138. Thomas WE, Trintchina E, Forero M, Vogel V, Sokurenko EV. 2002. Bacterial adhesion to target cells enhanced by shear force. *Cell* 109:913–23
139. Tondon A, Hsu H-J, Kaunas R. 2012. Dependence of cyclic stretch-induced stress fiber reorientation on stretch waveform. *J. Biomech.* 45:728–35
139a. Trappmann B, Gautrot JE, Connelly JT, Strange DGT, Li Y, et al. 2012. Extracellular-matrix tethering regulates stem-cell fate. *Nat. Mater.* 11:642–49
140. Vogel V, Sheetz M. 2006. Local force and geometry sensing regulate cell functions. *Nat. Rev. Mol. Cell Biol.* 7:265–75
141. Wang H, Ji B, Liu XS, Guo XE, Huang Y, Hwang K-C. 2012. Analysis of microstructural and mechanical alterations of trabecular bone in a simulated three-dimensional remodeling process. *J. Biomech.* 45:2417–25
142. Wang H, Ji B, Liu XS, van Oers RFM, Guo XE, et al. 2014. Osteocyte-viability-based simulations of trabecular bone loss and recovery in disuse and reloading. *Biomech. Model. Mechanobiol.* 13:153–66
143. Wang JH, Goldschmidt-Clermont P, Wille J, Yin FC. 2001. Specificity of endothelial cell reorientation in response to cyclic mechanical stretching. *J. Biomech.* 34:1563–72
144. Wang N, Naruse K, Stamenovic D, Fredberg JJ, Mijailovich SM, et al. 2001. Mechanical behavior in living cells consistent with the tensegrity model. *PNAS* 98:7765–70
145. Wang N, Tolić-Nørrelykke IM, Chen J, Mijailovich SM, Butler JP, et al. 2002. Cell prestress. I. Stiffness and prestress are closely associated in adherent contractile cells. *Am. J. Physiol. Cell Physiol.* 282:C606–16
146. Weng S, Fu J. 2011. Synergistic regulation of cell function by matrix rigidity and adhesive pattern. *Biomaterials* 32:9584–93
147. Wolfenson H, Henis YI, Geiger B, Bershadsky AD. 2009. The heel and toe of the cell's foot: a multifaceted approach for understanding the structure and dynamics of focal adhesions. *Cell Motil. Cytoskelet.* 66:1017–29
148. Wozniak MA, Chen CS. 2009. Mechanotransduction in development: a growing role for contractility. *Nat. Rev. Microbiol.* 10:34–43
149. Xiao T, Takagi J, Coller BS, Wang J-H, Springer TA. 2004. Structural basis for allostery in integrins and binding to fibrinogen-mimetic therapeutics. *Nature* 432:59–67
149a. Yu C-H, Law JBK, Suryana M, Low HY, Sheetz MP. 2011. Early integrin binding to Arg-Gly-Asp peptide activates actin polymerization and contractile movement that stimulates outward translocation. *PNAS* 108:20585–90
150. Zaidel-Bar R, Itzkovitz S, Ma'ayan A, Iyengar R, Geiger B. 2007. Functional atlas of the integrin adhesome. *Nat. Cell Biol.* 9:858–67
151. Zamir E, Katz BZ, Aota S, Yamada KM, Geiger B, Kam Z. 1999. Molecular diversity of cell-matrix adhesions. *J. Cell Sci.* 112:1655–69
152. Zamir E, Katz M, Posen Y, Erez N, Yamada KM, et al. 2000. Dynamics and segregation of cell-matrix adhesions in cultured fibroblasts. *Nat. Cell Biol.* 2:191–96
153. Zhong Y, He S, Dong C, Ji B, Hu G. 2014. Cell polarization energy and its implications for cell migration. *C. R. Mec.* 342:334–46
154. Zhong Y, He S, Ji B. 2012. Mechanics in mechanosensitivity of cell adhesion and its roles in cell migration. *Int. J. Comput. Mater. Sci. Eng.* 1:1250032
155. Zhong Y, Ji B. 2013. Impact of cell shape on cell migration behavior on elastic substrate. *Biofabrication* 5:015011

156. Zhong Y, Ji B. 2014. How do cells produce and regulate the driving force in the process of migration? *Eur. Phys. J. Special Top.* 223:1373–90
157. Zhong Y, Kong D, Dai L, Ji B. 2011. Frequency-dependent focal adhesion instability and cell reorientation under cyclic substrate stretching. *Cell. Mol. Bioeng.* 4:442–56
158. Zhu C, Lou J, McEver RP. 2005. Catch bonds: physical models, structural bases, biological function and rheological relevance. *Biorheology* 42:443–62
159. Ziegler WH, Gingras AR, Critchley DR, Emsley J. 2008. Integrin connections to the cytoskeleton through talin and vinculin. *Biochem. Soc. Trans.* 36:235–39